

SIMRAC

Final Project Report

**Title: THE DETERMINATION OF JOINT STIFFNESS TO IMPROVE
NUMERICAL MODELLING METHODS FOR DESIGNING
SAFER MINING PROCEDURES**

Author/s: R EVE and N C GAY

Research

Agency: CSIR MININGTEK

Project No: GAP 101

Date: NOVEMBER 1994

THE DETERMINATION OF JOINT STIFFNESS TO IMPROVE NUMERICAL MODELLING
METHODS FOR DESIGNING SAFER MINING PROCEDURES

R Eve and N C Gay
Rock Engineering
CSIR : Division of Mining Technology

1 **INTRODUCTION**

The rock mass surrounding mining excavations is transected by planes of potential weakness which, for the purposes of this study, shall be referred to as joints. Joints may be classified into two broad classes, those formed as a result of geological processes during the formation of the strata, the emplacement of igneous rock, or by subsequent tectonic activity. Examples of these joints include shrinkage joints, sheet joints and tectonic joints. The morphology of these planes of weakness varies from undulating to planar. Those associated with strata formation are generally planar to undulating, with a relatively large wavelength, and are essentially parallel to the general stratigraphy. Joints associated with igneous activity are mostly planar and result from cooling of the molten igneous rock; these joints are frequently filled with material such as quartz or calcite, as in the hangingwall lavas of the Ventersdorp Contact reef.

Mining-associated fractures or joints form as the result of stresses induced around the excavations and tend to follow the stress trajectories. Subsequent movement on these surfaces results in attrition of the rock surface creating weaknesses in the rock mass.

Joints are probably the most ubiquitous structures, found both in the natural and mining environment and it is generally accepted that they form as a result of rock strain due to in situ stresses, resulting in brittle fracture (Pollard and Aydin, 1988). This correlation between stress and strain enables joints to be important tools for inferring the in situ state of stress and the mechanical properties of the rock. By determining the relative ages of joints, different phases of brittle deformation can be mapped with respect to parameters, such as time, and in mines, face advance rate and geometry of the mining excavation. Price (1966) gives a detailed account of the theories of fault and geological joint development in brittle and semi-brittle rock. However, a detailed understanding of the development of mine induced fracturing has not as yet been established.

The behaviour of joints under various conditions of stress and strain depends largely on their origin and the history of deformation and stress to which they have been subjected. Much of the joint behaviour can be traced to mechanisms active at a microscopic scale. While an understanding of such microscopic mechanisms is often useful, it is the macroscopic behaviour of joints that is of primary interest to rock mechanics engineers. The macroscopic behaviour can be described in terms of measurable properties that can be related to various simplified models of joint behaviour. Often, the behaviour of jointed rock cannot be attributed to the properties of single joints but is the result of the interaction of many planes of weakness. Joint properties may sometimes be adjusted to take into account the effect of this interaction. The frequency, distribution and size of joint planes in relation to the size of test samples also plays an important role in the determination and use of joint properties.

The motivation for this project is the need to improve the ability of mining industry personnel in the use of numerical modelling techniques to enhance understanding of the behaviour of jointed rock and its influence on mine excavations. The presence of discontinuities accounts for much of the observed behaviour. In current modelling practice all discontinuities, be they fractures, geological joints, dykes or faults, are generally treated similarly and collectively referred to as joints. In this review it is intended to focus on the morphology of both geological and mining induced joints, methods for quantifying the parameters which control the in situ movement along joint planes and the application of this information to improving numerical models used for simulating the behaviour of the rock mass around mine excavations.

The modelling of a jointed rock mass takes one of three basic forms: the rock may be modelled as a continuum, it may be modelled as a continuum with some discrete discontinuities explicitly included, or the true discontinuous nature of the rock may be represented with a full discontinuum model.

The continuum approach relies on the assumption that joints are relatively short and their spacing is small in comparison to the dimensions of the model. The complexity of the continuum models for rock, ranges from the simple elastic laws, often with elastic moduli degraded to account for the presence of discontinuities, to complex, elasto-plastic and damage models with their associated yield criteria and flow laws. The orientation of discontinuities is not taken into account in most of these models, although some allow for orthotropic or fully anisotropic constitutive behaviour. However, ubiquitous joint models, which account for orientation, are used fairly widely.

The continuum approach has been used extensively; a review of the considerable volume of literature on this subject is not included in this report. Some discussion of the use of continuum models for jointed rock is to be found in Blanford and Key (1987b), Kazakids and Diederichs (1993), Pande, Beer and Williams (1990) and Hoek and Brown (1982).

The inclusion of discrete discontinuities in a continuum model requires introduction of a constitutive law to govern the behaviour of the joints. Discrete discontinuities are included because they are assumed to have a marked influence on the behaviour of the rock mass surrounding mine openings. It is usually only the most persistent of discontinuities that can be singled out as having a dominant influence; bedding planes, stress-induced fracturing and faults are typical examples of joints that may be treated in this way. These types of discontinuity do not fit the basic assumption used in continuum modelling of jointed rock. Having identified those joints which are most likely to influence the behaviour of the rock mass it becomes important that the behaviour of these joints is adequately represented.

The modelling of highly discontinuous systems is receiving increasing attention as computer hardware improves. In this approach many joints are explicitly defined. The model of the rock mass then consists of many small blocks formed as a result of the intersection of joints. While, in theory, all discontinuities can be included, in practice, some simplification of the pattern of discontinuities is necessary. The behaviour of the discontinuum model relies heavily on the constitutive relationships representing the behaviour of the different joints used. The study of full discontinuum models is still in its infancy compared with that of the continuum approaches described above. At this stage, emphasis is placed on qualitative rather than on quantitative results, hence at present there is little need for great accuracy in joint model parameter values. Of greater importance is the need for good qualitative representation of the behaviour of joint structures and hence their influence on the behaviour of the rock mass. Ultimately the behaviour of a discontinuum relies on competition between mechanisms of joint displacement and block rotation. As understanding of the application of the techniques for analysing models of this type increases, the need for accurate joint properties will become more important.

2 GEOMETRY AND FORMATION OF JOINTS

Joints are approximately planar discontinuities resulting from brittle deformation. Blocks of rock traversed by joints often become displaced relative to one another across these narrow discontinuities. Most are formed by fracturing, i.e., by development of cracks across which the original cohesion is lost. However, they may subsequently be healed by introduction of

secondary mineralization or recrystallization. Generally joints occur as families of fractures or joint sets which are regularly spaced through the rock mass and which have a common origin.

The majority of natural joint sets encountered in South African mines are either of sedimentary, igneous or tectonic origin. Joints of sedimentary origin generally form parallel to bedding or stratification, as a response to a reduction in the vertical stress due to erosion, or, in deep mines as a result of stress relief during mining activity. Stress induced fracturing of the rock mass as a result of mining in highly stressed ground also results in what are effectively jointed rock masses. In this situation the induced "joints" are generally parallel to each other, are regularly spaced and have the potential to act as planes of weakness across which displacement can occur and from which falls of ground can happen, particularly if geological joints or planes of weakness are able to interact with the stress induced fractures.

In order for the mechanisms of joint deformation and failure that lead to falls of ground to be analysed with numerical modelling tools, it is essential to include the active joints explicitly. Continuum models smear the influence of joints and only the roughest of assessments of the stability of the skin of an excavation can be obtained by numerical analysis. Such assessments are based on the extent of plastic strain or damage of the rock continuum, whereas the analysis of discontinuum models provides a direct assessment of joint movements and block stability.

Some simplification of the geometry of explicitly defined joints is required for discontinuum modelling, however the process of deriving suitable joint patterns from physical observations and measurements is complex. The specific objectives of a given analysis may influence the choices that have to be made. Development of an adequately representative, yet practically simple discontinuum model, is an art that is developing slowly as experience in the use of discontinuum models widens. The representation of 3D joint systems in 2D is not always possible. The need for simplicity in 3D models is necessary as computer resources can rapidly be exhausted with the additional storage and calculation requirements of a 3D analysis. The problem of providing an adequate joint pattern is greatly increased in complexity when a third dimension is considered. Some work has been done on methods to assist in establishing suitable 3D representations of rock joint patterns, see e.g. Kulatilake, Wathugala and Stephansson (in press) in which eight joint geometry modelling schemes are suggested and reference is made to a number of papers which deal with methods for the determination of joint geometry by physical observation, stochastic analysis and numerical simulation.

Currently in the SA mining industry, with the exception of the program DIGS (Napier and Hildyard 1992), there is limited access to numerical modelling tools which are capable of both predicting the formation of fractures and analysing the resulting discontinuous rock mass. It should be noted that significant advances in addressing this problem have been made in recent years (Owen, Munjiza, Owen and Bicanic 1992) and commercial software is currently in development. It is however possible to go some way to overcoming this problem by using currently available discontinuum modelling techniques. Fracturing may be represented by appropriate choice of joint model and parameters, these being applied to predefined, potential fractures in the model. It is important that those "joints" representing potential fractures which do not fail, should have no effect on the behaviour of the discontinuum. The major draw backs of this approach are, firstly, that fracture orientations are predefined and secondly that reasonably large numbers of incipient fractures need to be included in a model. Further development of this technique is necessary.

3 JOINT STIFFNESS

The "stiffness" of a joint depends to a large extent on the surface morphology or "ornamentation" of the joint surfaces. Common textures observed on joint surfaces, include "hackle marks" "rib marks", "feather" or "plumose river lines", and conchoidal rib marks. The topography of these structures can vary from planar surfaces to large deviations from the parent surface. In general the stiffness of a joint will depend on both the irregularities in the joint surface and the effective mating of the surfaces. A further factor to be considered is the interaction between joint sets, which if orientated at orthogonal or high angles to each other, can result in joint interlocking. This in turn would result in an increase in the overall resistance of the rock mass to movement along the major joint sets.

Other parameters which can affect the stiffness include: the infilling within joints and its thickness and cohesion properties, the initiation and propagation of new joint surfaces as a result of changes in the in situ stress field, for example due to a change in mining direction, and the degradation of existing joint strength properties as a result of weathering effects, removal of mineral infillings and minor slippage causing degradation of joint surfaces and the formation of powdered rock on joint surfaces.

A general form of the definition of joint stiffness is given by

$$\begin{pmatrix} d\sigma_n \\ d\sigma_s \end{pmatrix} = \begin{bmatrix} k_{nn} & k_{ns} \\ k_{sn} & k_{ss} \end{bmatrix} \begin{pmatrix} du_n \\ du_s \end{pmatrix}$$

where

$d\sigma_n$ and $d\sigma_s$ are changes in normal and shear stresses acting on the joint, du_n and du_s are changes in relative normal and shear displacements across the joint, and k_{nn} , k_{ss} , k_{ns} , and k_{sn} are stiffness terms.

In most joint models the diagonal terms in the stiffness matrix on the right hand side of this expression are assumed to be zero (Bandis 1990b, Plesha 1987 and Snyman 1991). An exception is the approach of Amadei and Saeb (1990). Hence, joint stiffness is essentially comprised of two parts: shear stiffness $K_s = k_{ss}$, or resistance to shearing or sliding of joint surfaces past each other, and the normal stiffness $K_n = k_{nn}$, acting at right angles to the joint surfaces. These stiffness terms are illustrated in the simple diagram given in Figure 3.1.

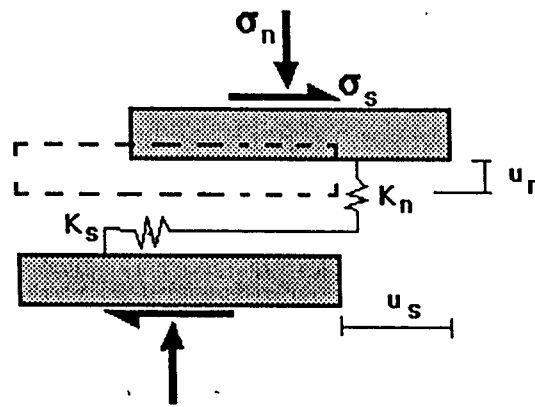


Figure 3.1 Normal and shear stiffness

The shear stiffness is generally highly variable, and difficult to predict (Brady and Brown 1985), whereas the normal stiffness is strongly stress dependent. This dependence is found to be highly nonlinear for a wide range of natural unfilled joint types (Snyman 1991).

Joint behaviour is strongly path dependent, that is, it is dependent on the history of loading and deformation. A time like parameter, t , is used to define the loading path stiffness and is evaluated at fixed times. In general the values of K_n and K_s are dependent on parameters which evolve with ..., for example the total slip undergone by the joint. The joint model determines the variation of stiffness with It should be noted that stiffness is usually derived by inversion of the compliance matrix, which is determined by the usual testing procedures.

3.1 Normal Stiffness

The non-linearity of the relationship between normal stress and normal displacement is attributed to some mismatching of the surface asperities as a result of high normal stresses, or due to slip on the joint surface, or a combination of these effects. The initial aperture and stress level are therefore basic factors in determining the normal stiffness behaviour during subsequent loading. The surface roughness and rock type also play a role (Bandis 1990a).

The typical nonlinear normal stress-closure behaviour during a single cycle of loading, as is shown in Figure 3.2, is described by Snyman (1991) as follows:

Upon initiation of loading, the joint closes rapidly as asperities readjust to their initial seating condition. As the normal stress increases and the initial seated position is taken up, further closure depends almost exclusively on the deformation of asperities. The tight mechanical interlocking between asperities at high normal stress, as well as the increased actual contact areas, creates a very effective confined environment, thus stiffening the deformational response of the joint. Upon subsequent unloading, the joint responds in an hysteretic and inelastic manner, with some permanent or irrecoverable, closure.

A variety of constitutive equations and experimental measurements relating normal stress and closure have been proposed and described in the literature some examples of which are reviewed by Bandis (1990a), see also Archambault et al (1990), Amadei and Saeb (1990) and Jing et al (1993). These examples are not discussed in detail because, for the purposes of numerical modelling, normal stiffness is often assumed constant. This assumption is easily justified since the range of closure over which non-linearity of normal stiffness is observed, is generally extremely small relative to the displacements which are of interest. Moreover, the normal displacements and stiffness usually play a role in the contact algorithm used to control the degree of interpenetration of joint surfaces that takes place as a result of numerical procedures used to analyse the interaction of the two sides of explicitly defined joints. Contact algorithm issues usually dominate the choice of normal stiffness values (see e.g. FLAC and UDEC program manuals).

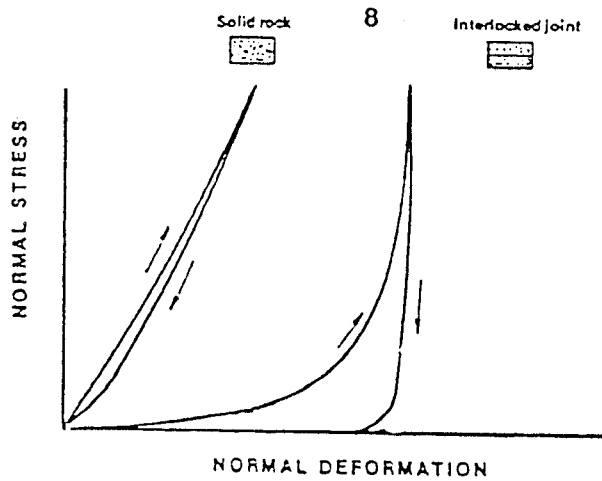
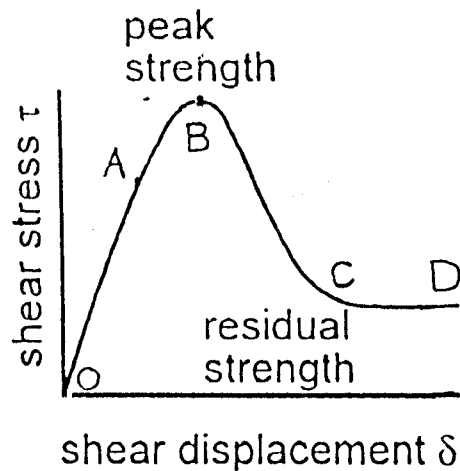


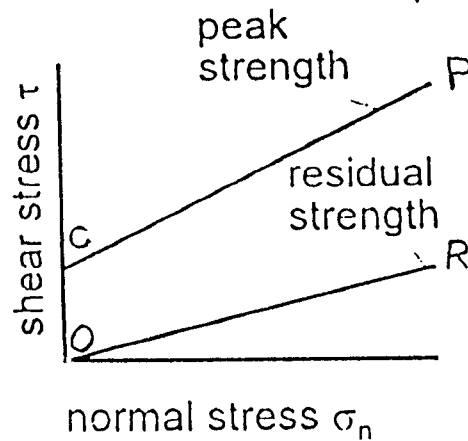
Figure 3.2 Normal stress vs closure behaviour (Bandis 1990a)

3.2 Shear stiffness

The two diagrams shown in Figure 3.3 provide a simple illustration of the typical features of rock joint shear behaviour.



a) Variation of shear stress with shear displacement



b) Variation of peak and residual strength with normal stress

Figure 3.3 Typical rock joint shear behaviour (Hoek, Kaiser and Bawden 1993)

These simple illustrations apply where shear is unidirectional; a more complicated picture is required to illustrate the effects of shear reversals and cyclic loading, these aspects of joint behaviour are described later.

Differentiating the curve in Figure 3.3 (a) gives joint stiffness. The fact that K_s goes negative indicates that joint behaviour is always potentially unstable. In most joint models, behaviour is assumed to be elastic initially. The maximum elastic shear displacement at A is very small and is usually insignificant in the context of numerical modelling. The shear stiffness in this region is constant and its value is often chosen on the basis of issues concerned with the stability of the numerical method used in the analysis of the models, rather than on the basis of physical measurements. At point A the joint yields and slip takes place. This point is determined by some form of initial shear strength criterion. Some hardening of the joint may occur between A and B, where the maximum, or peak, shear resistance of the joint is reached. In many models, hardening is not accounted for and the initial and peak shear strength of the joint are the same. BC represents a decay in the shear resistance of the joint. The micro processes which give rise to this decay in strength are often complicated. Physical measurement of this post peak phase of joint behaviour is the most difficult part of joint testing. The decay of joint strength may be the result of smoothing out the surface asperities, a process which eventually produces smooth joint surfaces which offer some residual resistance, CD in Figure 3.3 (a) and which is quantified in terms of a residual friction angle ϕ_r .

Physical measurements indicate that the residual friction angle is usually lower than the peak value. Experimental measurements indicate that friction angles and cohesion values vary with σ_n , in which case lines CP and OR in Figure 3.3 (b) are better represented by curves.

Much of the research work on joint models is concerned with providing an adequate description of the way in which the frictional and cohesive components of joint strength evolve after the initial peak strength of the joint has been exceeded. For the purposes of understanding shear, the basic friction angle, ϕ_b , is often used and is approximately equal to the residual friction angle. The basic friction angle is measured for ideal smooth surfaces of a given rock type.

A significant component of joint behaviour is dilation. Much of the complexity of joint modelling is associated with accounting for dilation in a realistic way. Dilation is usually described in terms of an angle, the dilation angle. The dilational aspects of joint behaviour become particularly complex where shear reversals take place. (Snyman 1991).

Figure 3.4 shows the shear response of a joint subjected to cyclic loading. The most important feature of this diagram is the difference between the shear resistance at initial slip for the first cycle and that slip at subsequent normal and reverse phases of the loading. This behaviour is not captured by many of the joint models currently in use. While purely cyclic loading is not of great importance in many of the models used by rock mechanics engineers, there are often situations where shear reversals are possible. For example during shear reversal joints may first dilate but then contract when the shear direction is reversed. This is generally attributed to joint surface asperities, damage to these asperities, and the changes resulting from the dilation/contraction behaviour of the joints.

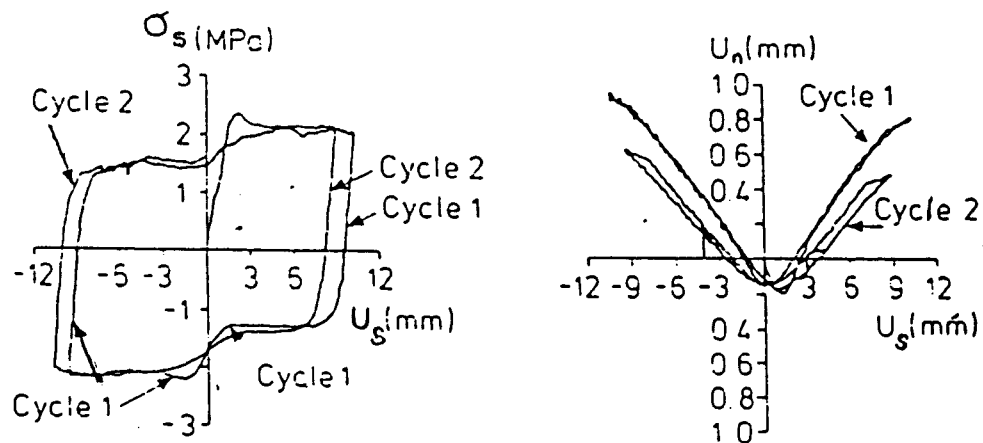


Figure 3.4 Joint behaviour under cyclic loading (Jing et al.)

Several researchers have performed extensive tests on the behaviour of joints under cyclic loading; and some have developed models which account for the observed behaviour. These include the models of Desai and Fishman (1991), which will be discussed in more detail later, and that of Jing Stephansson and Nordlund (1993). Jing et al's model was implemented in a version of UDEC, which is not commercially available. The model is based on the theoretical formulation of Plesha (1987) and makes use of empirical relations for work-strengthening, work weakening, variable stiffness parameters, surface degradation and different rates of dilatancy and contraction at different stages of shearing. The major downfall of the model is that it requires a large number of material parameters, some of which have to be determined by a "trial-and-error" process. The model also only works well for problems in which the shear displacement is less than the length of the primary

asperities, since joint dilatancy is not well defined at greater displacements. Consequently there is no joint model currently available to rock engineers in the SA mining industry which adequately takes cyclic and shear reversal behaviour into account. However, DIGS can model both forward and reverse slip with variable specified dilation angles (Napier and Hildyard 1992) but only allows for infinite joint stiffness. In practice it would seem that modelling a single reversal is adequate for incremental mining applications.

In the above discussion of the shear resistance of joints, attention has been restricted to their behaviour under quasi-static conditions. The response of joints under dynamic deformation and loading conditions involves further phenomena, in particular slip-stick behaviour. Slip-stick is the term used to describe instabilities in joint shear resistance. The phenomenon is often observed in direct shear tests where shear load may drop with an audible pop. Such unstable behaviour is of great interest in rock engineering as it offers a possible source mechanism for mining induced seismicity.

The difference between static and dynamic friction angles forms the basis for traditional methods for analysing slip-stick behaviour. Mechanisms associated with asperity failure have also been proposed. Slip-stick behaviour is thought to be the consequence of a nearly instantaneous drop in the joint shear strength which occurs as the joint starts to slip. Although it is known that the friction angle is a highly non-linear function of velocity, in conventional slip-stick analyses it is approximated by a step function. The elastic strain energy stored prior to the initiation of slip, becomes unbalanced when the friction angle drops to its dynamic value and as a result the joint surfaces accelerate with respect to one another. Slip stops once the energy balance is restored.

Considerable effort has been focussed on the analysis of slip-stick phenomena in recent years and a number of modifications to classical approaches have been proposed, see for example Bro (1992a) where asperity creep is included to improve the model. Other developments in the modelling of slip are discussed in Bro (1992b) and Lorig and Hobbs (1990).

The effect of infilling materials in joints such as fault gouge, silt and low friction materials such as chlorite or serpentine as well as joint healing materials such as quartz or calcite is to aggravate predictions of the likely response of joints subjected to shear or normal forces.

However, Ladanyi and Archambault (1977) were able to draw the following conclusions from a series of carefully designed laboratory studies:

- i) For most filled discontinuities the peak strength envelope lies between that for the filling material and that for a similar clean discontinuity;
- ii) The stiffnesses and shear strength of a filled joint surface decrease with infilling thickness, but are greater than the stiffnesses of the filling material;
- iii) The shear stress-displacement curves of filled discontinuities may reflect both the deformability of the filling material before the bounding rock surfaces make contact, and the deformability and shear failure of the rock asperities in contact;
- iv) The shear strength of a filled discontinuity is not necessarily dependent on the thickness of filling. If the discontinuity surfaces are flat and the infilling material has a low coefficient of friction, shearing takes place at the infill-rock contact.

These observations do not lend themselves readily to describing the response of a joint discontinuity and it is necessary to quantify them by developing a model which can describe the complete shear behaviour of the material.

4 MODELS FOR JOINT BEHAVIOUR

The simplest form of joint model used in practice is the Mohr-Coulomb model which is expressed as

$$\sigma_s = \sigma_n \tan \phi + c$$

where σ_s is the shear stress,
 σ_n is the normal stress,
 ϕ is the friction angle, and
 c is the joint cohesion

This expression is represented by CP in Figure 3.3 (b). In this simple form of joint model both ϕ and c are independent of normal stress. The term cohesion is derived from soil mechanics where the Mohr-Coulomb model was developed; in rock mechanics cohesion refers to the initial strength of a joint, which is based on surface roughness, rock strength and other factors. In this most basic form, the Mohr-Coulomb model gives only the initial

In spite of the gross simplifications inherent in its derivation, the Mohr-Coulomb model of joint behaviour is probably the most widely used. The main reason for its popularity is that only two simple quantities are required (ϕ and c); furthermore, due to the extent of this approximation there is little need for great accuracy in the measurement of these quantities and hence simple testing methods can be used.

Joint surface roughness is widely accepted to be the single most significant parameter influencing joint behaviour. Patton (1966) demonstrated this in shear, by using saw tooth specimens' Figure 4.1. This idealisation of a joint surface accounts to some extent for dilation during movement across shear planes and forms the basis for a large number of joint models.

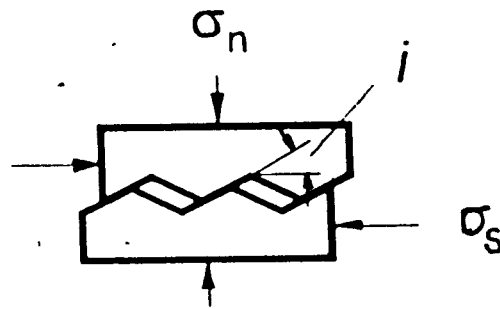


Figure 4.1 Saw-tooth model

Saw-tooth models are characterised by a condition of the form.

$$\sigma_s \leq \sigma_n \tan (\phi_b + i)$$

where ϕ_b is the basic friction angle, (ϕ_r may be used) and i is the angle of the saw tooth asperities.

This condition is only valid for joints subjected to low normal stress in high strength brittle rocks. At higher normal stresses brittle failure of the asperities takes place while in ductile rock types, plastic deformation of the asperities takes place.

Several approaches are used to derive detailed joint models from these simple concepts. One approach is to derive an elasto-plastic constitutive law for joint behaviour which includes suitable evolution laws for the degradation of asperities, and which can be used to evaluate expressions for dilation and shear stiffness. Examples of plasticity models for joints are described briefly below. Some joint models have been derived without specific reference to either the saw-tooth or plasticity concepts and an example, the continuously yielding joint model, is also described. Empirically determined relationships between joint roughness, rock strength and normal stress can be used to develop joint models. This is the approach which has been successfully followed by Barton and his co-workers (e.g. Barton and Choubey 1977). Much of the published experimental data about joint behaviour is analysed using the well known Barton-Bandis model. This model is described in some detail later.

4.1 Joint Models Based on the Theory of Plasticity

We first describe the basic framework of plasticity formulations and then describe some examples of elasto-plastic joint models.

The theory of plasticity formally sets out the form taken by constitutive laws for path dependant behaviour. The fundamental components of the theory are:

- 1 the concept of a region of allowable elastic stresses bounded by a yield surface; plastic flow takes place when the stress $\sigma = \{\sigma_n, \sigma_s\}$ lies on the surface;
- 2 a description of the evolution of internal variables, $\lambda = \{\lambda_1, \lambda_2 \dots\}$, describing the state of the material, or for the case in point, the condition of the joint surface.

Typical internal variables for joint models include slip, u^p , irreversible closure, u_n^p , and hardening parameters.

Yielding is determined by a yield condition of the form

$$f(\sigma, \lambda) \leq 0 \quad \begin{array}{l} f < 0, \text{ no plastic flow } (\lambda = 0) \\ f = 0, \text{ yielding } (\lambda \neq 0) \end{array}$$

where $\dot{\lambda}$ is rate of change of λ (The yield surface is defined by $f = 0$) and a plastic potential $h(\sigma, \lambda)$ from which the evolution of the internal variable is derived

$$\dot{\lambda}_i = \frac{\partial h}{\partial \lambda_i} \Big|_{\lambda_j = \text{const}} \quad i \neq j$$

A plasticity law is described as being associative if the same functional is used for both the yield function and plastic potential. Plasticity models for joint behaviour are in general non-associative.

4.1.1 The Mohr-Coulomb Model

The Mohr-Coulomb model for joint behaviour is usually implemented as an elasto-plastic constitutive law. In the absence of dilation, the formulation of this law is one of associated plasticity.

The yield function is

$$f(\sigma_n, \sigma_s) = |\sigma_s| - \sigma_n \tan \phi - c$$

$$\begin{aligned} \text{where } \sigma_s &= K_s (u_s - u_s^p) \\ \sigma_n &= K_n u_n \end{aligned}$$

The yield surface, $f = 0$, is illustrated in Figure 4.2. The evolution laws for slip on the joint is

$$\dot{u}_s^p = \alpha \frac{\sigma_s}{|\sigma_s|}$$

where α is a plastic multiplier which is always positive.

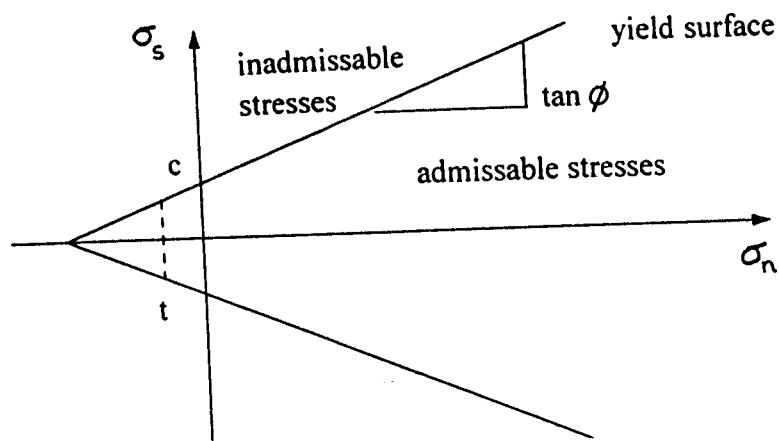


Figure 4.2 The yield surface for the Mohr-Coulomb joint constitutive model
 c = cohesion, t = tensile cut off

Dilation is taken to be the plastic part of normal closure u_n^p . An associative form of the Mohr-Coulomb constitutive law gives a dilation of $\tan \phi$, this is not a good representation. Physically reasonable formulations of the dilational response of a joint requires the introduction of an appropriate dilational term in the plastic potential from which plastic flow is derived. Implementations of the Mohr-Coulomb joint constitutive models which account for dilation are thus non-associative. (Plesha 1987). Dilation is often ignored which also makes the law non-associative with dilation.

$$\sigma_n = K_n (u_n - u_n^p)$$

A simple form of the additional evolution law is given by

$$\dot{u}_n^p = \dot{u}_s^p \tan \psi$$

where ψ is fixed dilation angle. The saw-tooth concept is not used in deriving this model. Variation of ϕ , c and ψ can be included, through the introduction of further evolution laws. A tension cut off is usually added to the formulation.

4.1.2 "Cap" Models

The inclusion of a "cap" is a commonly used method to enhance plasticity-based models of joint behaviour. This approach is used to include the effects of high normal stress. The cap restricts the elastic region as is illustrated in Figure 4.3.

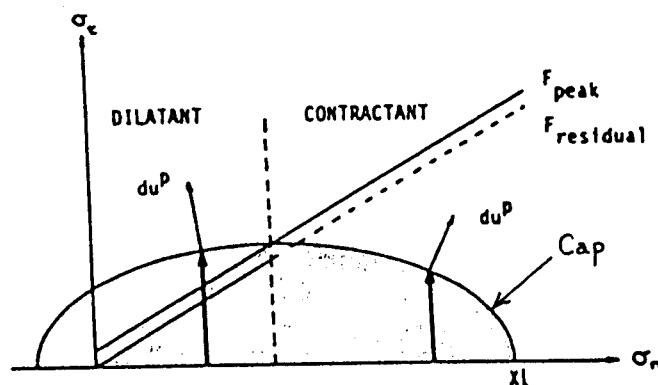


Figure 4.3 The yield surface for a "cap" model

An example of such a formulation is described by Kane and Drumm (1987) but the idea has been used by several authors. In their formulation, Kane and Drumm, model dilatancy and consequent strain softening is observed at high stress ratios σ_n/σ_s . The form of the cap was determined empirically from test data on joints collected in the Great Smoky Mountains of eastern Tennessee and western North Carolina. Normal plastic displacement representing dilation/contraction on the joint is given by

$$u_n^p = W (1 - e^{-Dx})$$

where the value of x is indicated in Figure 4.3, and D and W are material parameters.

W is the asymptote to the normal stress - normal displacement response as shown in Figure 3.2 and D is given by B/WE where $3 \leq B \leq .5$ and was found to give good results.

In this particular formulation of a "cap" model a reduction in cohesion is used so that two forms of the basic Mohr-Coulomb yield function are required.

$$f_{initial} = |\sigma_s| - \sigma_n \tan(\phi_{peak}) - C_{peak}$$

and

$$f_{residual} = |\sigma_s| - \sigma_n \tan(\phi_{residual}) - C_{residual}$$

The formulation models both dilatant and contractant response for a range of normal stresses but is best suited to applications involving low normal stresses.

A summary of material parameters used in this study are given in the following table.

	C peak	ϕ_{peak} (deg.)	C res (kPa)	$\phi_{res.}$ (deg.)	K_n (kN/m)	K_s (kN/m)	D (1/kPa)	W (cm)	R	E_i (kPa)	λ
Quartzite	-125	28	0.0	28	5e10	3e5	3e-3	5e-1	1.75	1100	200
Quartzite/ Siltstone	-50	32	0.0	32	10e6	5e5	5e-3	.01	.01	300	400

4.1.3 A General Plasticity Model

The framework of the theory of plasticity provides for the development of very general joint constitutive models which give better performance than those represented by either the

Mohr-Coulomb or cap models.

Desai and Fishman (1991) have developed a general, hierarchical approach for the constitutive modelling of joints within the context of plasticity theory. Their approach differs from that used to obtain "cap" models in that

- a) the yielding is described by a single continuously expanding function F
- b) the hardening or growth function is defined in terms of both shear and normal plastic displacements
- c) dilatant normal displacements before the peak, failure or ultimate state is reached (this is observed on many joints)
- d) the ultimate state is defined as the envelope of asymptotic stress values and contains previously used peak failure or critical states as special cases.

The model is evolved from a special case of general plasticity by substituting stress and deformation parameters for a joint in the place of analogous measures used in the full 3D continuum theory, these being σ_n , σ_s , u_n and u_s and

$$\begin{aligned}\xi &= \int_0^t [(du^p_s)^2 + (du^p_n)^2]^{1/2} dt \\ \xi_v &= \int_0^t [(du^p_s)^2]^{1/2} dt \\ \xi_d &= \int_0^t [(du^p_s)] dt\end{aligned}$$

the plastic trajectory, its volumetric and deviatoric parts respectively, and t is the loading path parameter.

The resulting yield function takes the simple form:

$$F(\sigma) = \sigma_s + \alpha \sigma_n^n - \gamma \sigma_n^2$$

When $\alpha = 0$, this represents the ultimate surface as is illustrated in Figure 4.4.

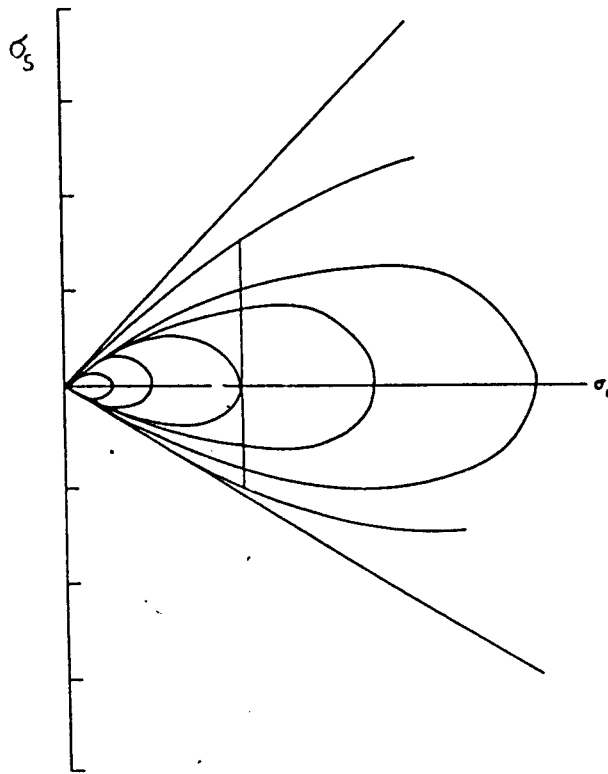


Figure 4.4 The yield function used by Desai and Fishman (1991)

An adjustment for finite tensile strength can be included by applying a shift to σ_n .

The plastic potential function used in this formulation is

$$Q(\sigma, \xi) = F(\sigma) + h(\sigma_n, \xi).$$

With h constant, the constitutive law is associative.

The function h is derived from the growth function for α and is given by

$$h(\sigma_n, \xi) = K(\alpha_1 - \alpha)(1 - \gamma_v) \sigma_n^\alpha$$

where

K is a material parameter

α_1 is the value α at the end of initial normal loading, and

$\gamma_v = \xi_v/\xi$.

A relatively small number of model constants are introduced. The determination of these is fully described. The parameter γ is derived from a least squares fit of peak shear stress obtained at various normal stresses. The power n is found by considering the stress state during shear where no change in normal displacement takes place and the growth function is characterised by the relation

$$\alpha = a\xi^b$$

where a and b are material parameters and are found by plotting $\log \alpha$ vs $\log \xi$ for shear tests under different σ_n . The parameter K is obtained by considering the relation between normal and shear displacements.

A series of quasi-static direct shear tests were performed for simulated (idealised, saw-tooth) joint surfaces. The model was verified with material constants determined from these tests as summarised in the following table.

Constant	Surface i				Average constants	Reverse loading $i = 9^\circ$
	Flat	5°	7°	9°		
γ	0.36	0.42	0.78	0.81	-	0.45
n	2	2.2	3	2.9	2.5	2.5
a	0.023	0.011	0.031	0.047	0.028	0.024
b	-0.116	-0.293	-0.223	-0.162	-0.199	-0.15
k	0.7	0.7	0.7	0.55	0.66	1.5

4.1.4 Other Elasto-plastic Joint Models

Plesha and co-workers (Plesha 1987, Plesha and Haimson 1988, and Qui, Plesha, Huang and Haimson 1993) have also developed a number of joint constitutive laws. These laws are based on careful description of micromechanisms of joint behaviour for joints with idealised surface profiles. The first model (Plesha 1987) is based on a saw-tooth asperity model, which, following later refinement, now allows for a sinusoidal asperity idealisation of the surface. A general theory is developed based on the assumption that displacements are additively composed of elastic and plastic parts and plastic deformation is additively composed by sliding and damage parts. The final constitutive model is referred to as the $\alpha - \gamma$ model. This model and derivations of it are particularly lengthy and complex and are not discussed further here. However, a number of model parameters are used and formulae for computing these from standard cyclic direct shear tests, are derived. The work includes

a fairly thorough experimental investigation of joint behaviour (Huang, Haimson, Plesha and Qui, 1993). Good representation of shear reversal and cyclic loading behaviour are achieved with the model.

Snyman (1991) paid special attention to the modelling of variations in dilation angles which occur with shear stress reversals. He developed three models, the first is based on a simple Coulomb friction model, the second is a saw-tooth asperity formulation and in the third, the asperity model is adapted by using a logspiral relationship to enhance the dependence of dilation on shear deformation. This work is aimed not only at improving the modelling capability of joint constitutive laws but also at deriving efficient algorithms for use in implicit finite element formulations.

Still further examples of elasto-plastic formulations of joint models are to be found in Aydan et al (1990), and Jing (1990). The formulation of joint models is very popular and compilation of a full list of such models is not easily achieved.

4.2 The Continuously Yielding Joint Model

The continuously yielding joint model proposed by Cundall and Hart (1984) is designed to reproduce the type of phenomena observed in shear experiments with rock joints such as post-peak softening and dilation. The formulation is intended to simulate the internal mechanism of progressive damage of the joint under shear, but is not based on either a classical asperity type model or a classical plasticity theory. Strength degradation of the discontinuity is assumed to be a function of displacement only. The formulation is obtained by choosing a mathematical expression which, given suitable values for governing parameters, produces curves similar to those obtained in experiments. Some of these parameters may be related to physically measurable joint properties. The concept of a bounding surface is used, the bounding strength being given by

$$\tau_m = \sigma_n \tan \phi_m \operatorname{sgn}(\Delta u_d)$$

where ϕ_m is the friction angle that would apply if the joint were to dilate at the maximum dilation angle. The friction angle is continuously reduced. The dilation angle is given by

$$\psi = \tan^{-1} \left(\frac{\sigma_s}{|\sigma_n|} \right) - \phi_b$$

The basic shear stress increment is calculated as

$$\Delta \sigma_s = F k_s \Delta u_s$$

where

$$F = \left(\frac{1 - \sigma_s / \gamma_m}{1 - r} \right)$$

The factor r is intended to restore the elastic stiffness immediately after shear reversal. In practice r is limited by numerical stability considerations.

The change in friction angle is given by

$$\Delta \phi_m = -1/R (\phi_m - \phi_b) \Delta u^p_s$$

where

$$\Delta u^p_s = (1 - F) \Delta u_s$$

Joint roughness is represented by R , however no correlation between this parameter and more widely used joint roughness characterisations appears to have been performed.

The continuously yielding joint model's shear stress-displacement curve and bounding strength are shown in Figure 4.5.

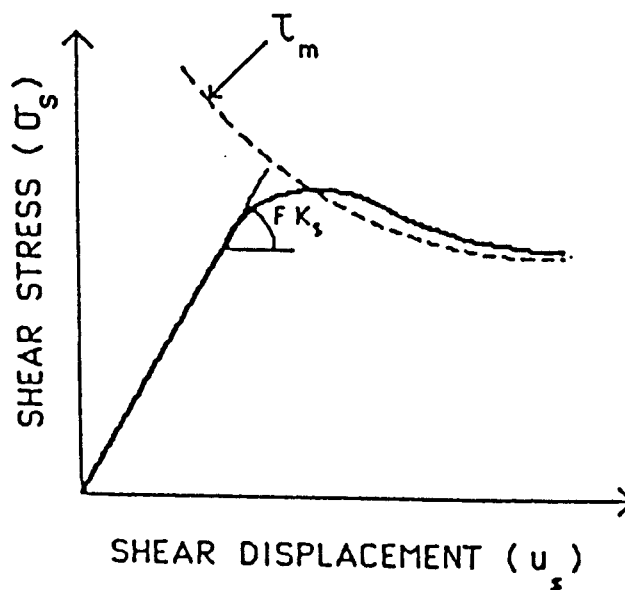


Figure 4.5 Continuously yielding joint model

The model allows for an exponential dependence of normal stiffness on normal stress, however there is no indication of how the required parameters should be obtained and in all documented applications of the model constant stiffness is used.

The continuously yielding model has been used to study fault stabilities by Cundall and Lemos (1990), with some success for very simplified model geometries. It has also been tested under cyclic loading but these tests do not extend to the point of reversed slip and hence it is not clear that the model will perform in such circumstances.

In spite of its shortcomings the continuously yielding joint model is perhaps the most sophisticated model in use in the SA mining industry; it is implemented in UDEC.

4.3 The Barton-Bandis Model

Barton and co-workers proposed the relationship

$$\sigma_s = \sigma_n \tan \left[\phi_b + JRC \log_{10} \left(\frac{JCS}{\sigma_n} \right) \right]$$

where JRC is the joint roughness coefficient

and JCS is the joint wall uniaxial compressive strength.

This model is essentially an extension of Patton's model with an additional asperity failure component. Values for JRC and JCS have been derived from many experimental measurements, and a scale of 0 to 20 for JRC includes both perfectly smooth and very rough joints. The model can be written in the form

$$\sigma_s = \sigma_n \tan(\phi_b + \mu)$$

where

$$\mu = JRC \log_{10} \left(\frac{JCS}{\sigma_n} \right)$$

which is the effective dilation angle. In this basic form no dependence on shear displacement is included and the model therefore only determines the peak shear strength of a joint.

In subsequent developments (Barton and Bakhtar, 1983), the concept of mobilised frictional resistance (mob) was introduced, and an expression for the evolution of mobilised friction with shear displacement was derived from a study of experimental results (Lechnitz, 1985).

These showed that the ratio $JRC_{(mob)}/JRC_{(peak)}$ could be correlated with $u_s/u_s(peak)$ to give the effective "mobilised friction angle" as

$$\phi_{mob} = \phi_b + JRC_{(mob)} \log_n \left(\frac{JCS}{\sigma_n} \right)$$

where

$$JRC_{(mob)} = A JRC_{(peak)}$$

The parameter A depends on the negative displacement $B = u_s/u_s(peak)$. The following linear extrapolations can be used between characteristic points of the $JRC(mob)/JRC(peak)$ vs $u_s/u_s(peak)$, model described by Barton et al (1985).

$0.0 < B \leq 0.3$	$A = 1$
$0.3 < B \leq 0.6$	$A = 2.5B - 0.75$
$0.6 < B \leq 1.0$	$A = 0.625B + 0.375$
$1.0 < B \leq 2.0$	$A = 0.15B + 1.15$ (8)
$2.0 < B \leq 4.0$	$A = 0.075B + 1.00$
$4.0 < B \leq 10.0$	$A = (-0.2B/6) + (5/6)$
$10.0 < B \leq 100.$	$A = (-0.5B/90) + (50/90)$

The basic expression for joint behaviour is rewritten as

$$\sigma_s = \sigma_n \tan (\phi_b + \mu)$$

where

$$\mu = JRC \log_{10} \left(\frac{JCS}{\sigma_n} \right)$$

and μ is the effective dilation.

A further refinement of the basic Barton-Bandis model concerns the variation of dilation angle (Barton and Choubey, 1977). A damage coefficient, M , is introduced in

$$\mu_{peak} = \frac{1}{M} JRC_{(peak)} \log_{10} \left(\frac{JCS}{\sigma_n} \right)$$

where $M=1$ at low values of σ_n and $M=2$ at high values. In recent work by Barton (1990) measurements of the variation in M have been made, which indicate that M asymptotically approaches a value of 4 to 5 for a JRC value of 10 to 12 and values of JCS/σ_n of 6 to 10. Further work is needed to improve understanding of the evolution of M for a variety of roughness and strength conditions.

The values of JRC and JCS have been shown to be scale dependant; discussion of the measurement and scaling of these parameters is included later in this report.

This empirically derived model can be recast in the form of an elasto-plastic constitutive mode (see Pande, Beer and Williams 1990). The yield function is given by:

$$F(\sigma) = |\sigma_s| + \sigma_n \tan \left(JRC \log_{10} \left(\frac{JCS}{\sigma_n} \right) + \phi_r \right)$$

and the plastic potential from which the evolution of dilation angle is derived is given by

$$Q(\sigma) = |\sigma_s| + \frac{\sigma_n \tan \lambda_2}{k_1} - \frac{JRC}{264} \frac{\sigma_n^2}{JCS}$$

where:

$$\begin{aligned} \lambda_1 &= JRC \log_{10} \left(\frac{JCS}{\sigma_n} \right) + \phi_r \\ \lambda_2 &= \lambda_1 - \phi_r \\ k_1 &= 1 - \tan \lambda_2 \tan \phi_r \end{aligned}$$

A form of the Barton-Bandis model is available in UDEC.

4.4 Other Joint Models

A similar model is the comprehensive discontinuity model of Roberds and Einstein (1978)

which consists of the following 4 relationships.

- i) σ_s vs σ_n - the failure characteristic (c, ϕ)
- ii) σ_s vs u_s - the shear stiffness (K_s)
- iii) u_s vs u_n^p - the asperity angle (i_r)
- iv) σ_n vs u_n^p - the normal stiffness (K_n)

where σ_s = shear stress, σ_n = normal stress; u_s = shear displacement, c = cohesion, ϕ = angle of sliding friction; and u_n^p = dilation.

Of the four relationships only 3 are required to describe the shear behaviour of a discontinuity.

Using this model, Lee (1983) was able to analyse the ground behaviour of a Crown Pillar at Mount Isa Mine and determine values of the sliding friction on coherent and slickensided bedding planes.

Characteristic properties of the weak bedding planes were:

- i) spaced ~ 4,5 m apart;
- ii) planar, slickensided and graphite coated;
- iii) angle of sliding friction of $\pm 10^\circ$ (minimum of $8,5^\circ$ for graphite coated planes) and an average angle of 20° for all bedding planes tested.

The most applicable relationship was found to be a modified version of Barton's (1976) formula.

The ultimate angle of sliding friction (i.e. lowest one measured in the laboratory, $8,5^\circ$ for graphitic bedding planes at Mount Isa) was used as the basic friction angle, but the main "modification" to Barton's formula was in letting JCS equal the shear strength of intact rock. In doing so, more realistic asperity angle values were predicted for very low and very high normal stresses (σ_n). However, to apply this technique the in situ stress state has to be known so that estimates of the in situ shear strength can be determined. This leads to a reconciliation of laboratory and in situ shear strength values.

Often parameters which were required included the in situ JRC, the asperity angle and the shear stiffness which encompasses both the pre- and post-yield stiffness values. Using Barton and Choubey's (1977) estimate that a displacement of about 1% of the test block length is required to reach peak shear strength, and knowing the nominal stresses acting on the bedding planes, Lee estimated that, depending on the separation between the bedding or shear planes, shear stiffness values were as follows:

MINING LAYOUT	BEDDING PLANE SPACING (m)	SHEAR STIFFNESS (GPa)
Cut and fill stope - crown pillar	± 0,1	8,5
	± 6,0	0,85
	± 5,0	0,3
Sub-level open stope: - fractures pillar	± 0,1	5,5
	± 6,0	0,5
	± 5,0	0,2

Lee also noted that after about 20 mm of shear slip on the bedding plane, sub-perpendicular cracks formed away from the footwall side of the bedding planes, causing slip on the plane to stop, and start on other planes, so that the blocks between active shear planes were rotated. The effect of this was to increase the roughness coefficient on the plane, ultimately stopping the shearing, and causing shear to be initiated on the closest and next weakest bedding plane.

Lee's paper has been dealt with in some detail because it highlights the problems encountered and the observations or measurements necessary in order to determine the parameters required to quantify the behaviour of the rock mass in mining situations and to obtain quantitative failure parameters for use in numerical modelling.

5 METHODS FOR ROCK MASS CLASSIFICATION

Tractable methods for determining the shear and normal strength characteristics of planar surfaces are Barton's "Q" method for determining rock mass characteristics and support requirements. (Barton et al, 1974) and Bieniawski's (1989) Rock Mass Rating systems.

- 5.1 The Q method is based on an evaluation of a large number of case histories from underground excavations which enabled the development of a "Tunnelling Quality Index" (Q) for determining rock mass characteristics and support requirements. The value of Q varies on a logarithm scale from 0,001 - 1 000 and is defined by:

$$Q = \frac{RQD}{J_n} \times \frac{J_r}{J_a} \times \frac{J_w}{SRF}$$

where	RQD	=	Rock quality designation
	J_n	=	Joint set number
	J_r	=	Joint roughness number
	J_a	=	Joint alteration number
	J_w	=	Joint water reduction number
	SRF	=	Stress reduction factor.

These parameters can be used to describe various aspects of the rock mass and its response to stress, as follows:

- i) RQD/J_n represents the structure of the rock mass block or particle size. The extreme values are 100/0,5 and 10/20, a factor of 400 difference.
- ii) J_r/J_a represents the roughness and friction characteristics of the joint walls or filling material, weighted in favour of rough unaltered joints. The strength is reduced when joints are filled with mineral coatings and is further reduced when no rockwall contact exists.
- iii) J_w/SRF is a complicated empirical factor which describes the "active stress". SRF is a measure of the loosening load acting on an excavation traversed by shear zones, and also of the rock stress in competent rock, and squeezing loads in very weak rock. Thus it can be regarded as a total stress parameter (Hoek et al. 1994, in press).

J_w is a measure of water pressure, which reduces the normal stress acting on joint sets, thus reducing the shear strength of the joints.

These three parameters are generally sufficient to provide a rough estimate of (i) block size, (RQD/J_n) (ii) interblock shear strength (J_r/J_a) and (iii) active stress (J_w/SRF) (Hoek et al,

1994).

To facilitate the application of the method Barton and his co-workers (1974) prepared a series of tables summarizing the application of the method as follows:

Table 5.1 Classification of individual parameters for Quality Index Q (after Barton et al. 1974)

DESCRIPTION	VALUE	NOTES	
1. ROCK QUALITY DESIGNATION	RQD		
A. Very poor	0 - 25	1. Where RQD is reported or measured as ≤ 10 (including 0), a nominal value of 0 is used to evaluate Q.	
B. Poor	25 - 50		
C. Fair	50 - 75	2. RQD intervals of 5, i.e. 100, 95, 90 etc. are sufficiently accurate.	
D. Good	75 - 90		
E. Excellent	90 - 100		
2. JOINT SET NUMBER	J_n		
A. Massive, no or few joints	0.5 - 1.0	1. For intersections use $(3.0 \times J_n)$ 2. For portals use $(2.0 \times J_n)$	
B. One joint set	2		
C. One joint set plus random	3		
D. Two joint sets	4		
E. Two joint sets plus random	6		
F. Three joint sets	9		
G. Three joint sets plus random	12		
H. Four or more joint sets, random, heavily joints, 'sugar cube', etc.	15		
J. Crushed rock, earthlike	20		
3. JOINT ROUGHNESS NUMBER	J_r		
<i>a. Rock wall contact</i>			
<i>b. Rock wall contact before 10 cm shear</i>			
A. Discontinuous joints	4	1. Add 1.0 if the mean spacing of the relevant joint set is greater than 3 m. 2. $J_r = 0.5$ can be used for planar, slickensided joints having lineations, provided that the lineations are oriented for minimum strength.	
B. Rough and irregular, undulating	3		
C. Smooth undulating	2		
D. Slickensided undulating	1.5		
E. Rough or irregular, planar	1.5		
F. Smooth, planar	1.0		
G. Slickensided, planar	0.5		
<i>c. No rock wall contact when sheared</i>			
H. Zones containing clay minerals thick enough to prevent rock wall contact	1.0 (nominal)		
J. Sandy, gravelly or crushed zone thick enough to prevent rock wall contact	1.0 (nominal)		
4. JOINT ALTERATION NUMBER	J_a	ϕ_r degrees (approx.)	
<i>a. Rock wall contact</i>			
A. Tightly healed, hard, non-softening, impermeable filling	0.75	1. Values of ϕ_r , the residual friction angle, are intended as an approximate guide to the mineralogical properties of the alteration products, if present.	
B. Unaltered joint walls, surface staining only	1.0		25 - 35
C. Slightly altered joint walls, non-softening mineral coatings, sandy particles, clay-free disintegrated rock, etc.	2.0		25 - 30
D. Silty-, or sandy-clay coatings, small clay-fraction (non-softening)	3.0		20 - 25
E. Softening or low-friction clay mineral coatings, i.e. kaolinite, mica. Also chlorite, talc, gypsum and graphite etc., and small quantities of swelling clays. (Discontinuous coatings, 1 - 2 mm or less in thickness)	4.0		8 - 16

Table 5.1 (continued)

DESCRIPTION	VALUE		NOTES
4. JOINT ALTERATION NUMBER	J_a	ϕ_r degrees (approx.)	
<i>b. Rock wall contact before 10 cm shear</i>			
F. Sandy particles, clay-free, disintegrating rock etc.	4.0	25 - 30	
G. Strongly over-consolidated, non-softening clay mineral fillings (continuous < 5 mm thick)	6.0	16 - 24	
H. Medium or low over-consolidation, softening clay mineral fillings (continuous < 5 mm thick)	8.0	12 - 16	
J. Swelling clay fillings, i.e. montmorillonite, (continuous < 5 mm thick). Values of J_a depend on percent of swelling clay-size particles, and access to water.	8.0 - 12.0	6 - 12	
<i>c. No rock wall contact when sheared</i>			
K. Zones or bands of disintegrated or crushed rock and clay (see G, H and J for clay conditions)	6.0		
L. Zones or bands of silty- or sandy-clay, small clay fraction, non-softening	8.0		
M. Zones or bands of silty- or sandy-clay, small clay fraction, non-softening	8.0 - 12.0	6 - 24	
N. Zones or bands of silty- or sandy-clay, small clay fraction, non-softening	5.0		
O. Thick continuous zones or bands of clay	10.0 - 13.0		
P. & R. (see G.H and J for clay conditions)	13.0 20.0		
5. JOINT WATER REDUCTION	J_w	approx. water pressure (Kgl/cm ²)	
A. Dry excavation or minor inflow i.e. < 5 l/n locally	1.0	< 1.0	
B. Medium inflow or pressure, occasional outwash of joint fillings	0.66	1.0 - 2.5	
C. Large inflow or high pressure in competent rock with unfilled joints	0.5	2.5 - 10.0	1. Factors C to F are crude estimates; increase J_w if drainage installed.
D. Large inflow or high pressure	0.33	2.5 - 10.0	
E. Exceptionally high inflow or pressure at blasting, decaying with time	0.2 - 0.1	> 10	2. Special problems caused by ice formation are not considered.
F. Exceptionally high inflow or pressure	0.1 - 0.05	> 10	
6. STRESS REDUCTION FACTOR		SRF	
<i>a. Weakness zones intersecting excavation, which may cause loosening of rock mass when tunnel is excavated</i>			
A. Multiple occurrences of weakness zones containing clay or chemically disintegrated rock, very loose surrounding rock (any depth)		10.0	1. Reduce these values of SRF by 25 - 50% if the relevant shear zones only influence but do not intersect the excavation.
B. Single weakness zones containing clay, or chemically disintegrated rock (excavation depth < 50 m)		5.0	
C. Single weakness zones containing clay, or chemically disintegrated rock (excavation depth > 50 m)		2.5	
D. Multiple shear zones in competent rock (clay free), loose surrounding rock (any depth)		7.5	
E. Single shear zone in competent rock (clay free). (depth of excavation < 50 m)		5.0	
F. Single shear zone in competent rock (clay free). (depth of excavation > 50 m)		2.5	
G. Loose open joints, heavily jointed or 'sugar cube', (any depth)			

Table 5.1 (Continued)

DESCRIPTION			VALUE	NOTES
6. STRESS REDUCTION FACTOR			SRF	
<i>b. Competent rock, rock stress problems</i>				
	σ_c/σ_1	σ_t/σ_1		2. For strongly anisotropic virgin stress field
H. Low stress, near surface	> 200	> 13	2.5	(if measured): when $5 \leq \sigma_1/\sigma_3 \leq 10$, reduce σ_c
J. Medium stress	200 - 10	13 - 0.66	1.0	to $0.8\sigma_c$ and σ_t to $0.8\sigma_t$. When $\sigma_1/\sigma_3 > 10$,
K. High stress, very light structure (usually favourable to stability, may be unfavourable to wall stability)	10 - 5	0.66 - 0.33	0.5 - 2	reduce σ_c and σ_t to $0.6\sigma_c$ and $0.6\sigma_t$, where
L. Mild rockburst (massive rock)	5 - 2.5	0.33 - 0.16	5 - 10	σ_c = unconfined compressive strength, and
M. Heavy rockburst (massive rock)	< 2.5	< 0.16	10 - 20	σ_t = tensile strength (point load) and σ_1 and
<i>c. Squeezing rock, plastic flow of incompetent rock under influence of high rock pressure</i>				
N. Mild squeezing rock pressure			5 - 10	σ_3 are the major and minor principal stresses.
O. Heavy squeezing rock pressure			10 - 20	3. Few case records available where depth of crown below surface is less than span width. Suggest SRF increase from 2.5 to 5 for such cases (see H).
<i>d. Swelling rock, chemical swelling activity depending on presence of water</i>				
P. Mild swelling rock pressure			5 - 10	
R. Heavy swelling rock pressure			10 - 20	
ADDITIONAL NOTES ON THE USE OF THESE TABLES				
When making estimates of the rock mass quality (Q), the following guidelines should be followed in addition to the notes listed in the tables:				
1. When borehole core is unavailable, RQD can be estimated from the number of joints per unit volume, in which the number of joints per metre for each joint set are added. A simple relationship can be used to convert this number to RQD for the case of clay free rock masses: $RQD = 115 - 3.3 J_v$ (approx.), where J_v = total number of joints per m^3 ($0 < RQD < 100$ for $35 > J_v > 4.5$).				
2. The parameter J_n representing the number of joint sets will often be affected by foliation, schistosity, slaty cleavage or bedding etc. If strongly developed, these parallel 'joints' should obviously be counted as a complete joint set. However, if there are few 'joints' visible, or if only occasional breaks in the core are due to these features, then it will be more appropriate to count them as 'random' joints when evaluating J_n .				
3. The parameters J_r and J_a (representing shear strength) should be relevant to the weakest significant joint set or clay filled discontinuity in the given zone. However, if the joint set or discontinuity with the minimum value of J_r/J_a is favourably oriented for stability, then a second, less favourably oriented joint set or discontinuity may sometimes be more significant, and its higher value of J_r/J_a should be used when evaluating Q. The value of J_r/J_a should in fact relate to the surface most likely to allow failure to initiate.				
4. When a rock mass contains clay, the factor SRF appropriate to loosening loads should be evaluated. In such cases the strength of the intact rock is of little interest. However, when jointing is minimal and clay is completely absent, the strength of the intact rock may become the weakest link, and the stability will then depend on the ratio rock-stress/rock-strength. A strongly anisotropic stress field is unfavourable for stability and is roughly accounted for as in note 2 in the table for stress reduction factor evaluation.				
5. The compressive and tensile strengths (σ_c and σ_t) of the intact rock should be evaluated in the saturated condition if this is appropriate to the present and future in situ conditions. A very conservative estimate of the strength should be made for those rocks that deteriorate when exposed to moist or saturated conditions.				

To facilitate further application of the Q method Barton and Choubey (1977) developed a set of standard joint roughness profiles, which could be correlated with corresponding JRC values. These are given in Figure 5.1. Subsequently Barton added to this. Figure 5.2 provides similar information but allows for the correlation between the joint roughness number J_r (see Table 5.1) and values of JRC in the Q system for samples ranging from 200 - 1 000 mm.

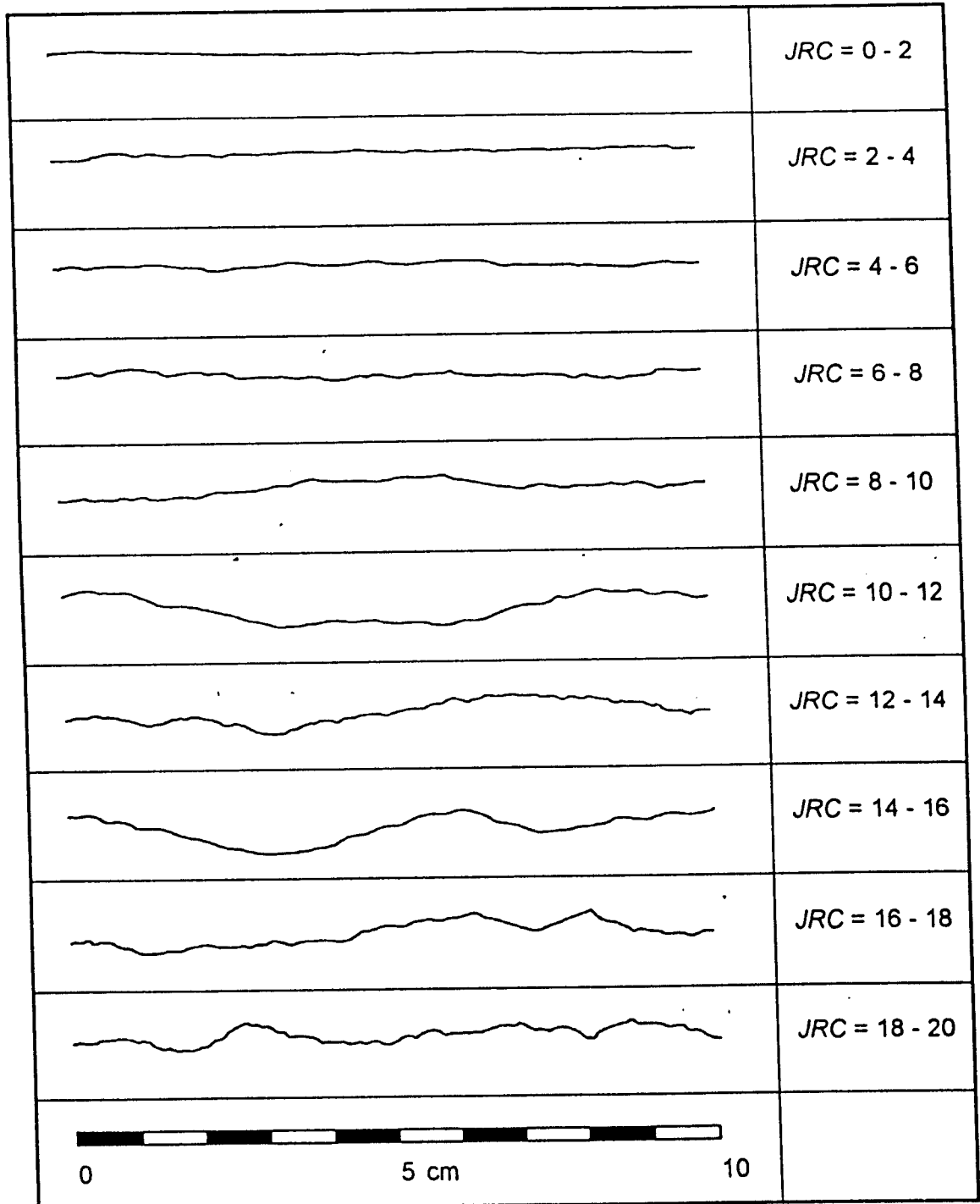


Figure 5.1 Roughness profiles and corresponding JRC values (After Barton and Choubey, 1977). Note profiles are reproduced at full scale so as to facilitate direct comparison with measured roughness profiles.


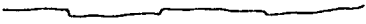

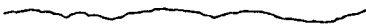

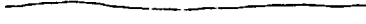
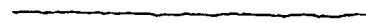
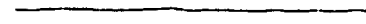

Description	Profile	J_r	JRC 200mm	JRC 1 m
Rough		4	20	11
Smooth		3	14	9
Slickensided		2	11	8
	Stepped	2	11	8
Rough		3	14	9
Smooth		2	11	8
Slickensided		1.5	7	6
	Undulating	1.5	7	6
Rough		1.5	2.5	2.3
Smooth		1.0	1.5	0.9
Slickensided		0.5	0.5	0.4
	Planar	0.5	0.5	0.4

Figure 5.2 Relationship between J_r in the Q system and JRC for 200 mm and 1 000 mm samples (After Barton, 1987). Note profiles are reproduced at full scale so as to facilitate direct comparison with measured roughness profiles.

A simple tilt test for estimating the joint roughness coefficient of matching planar surfaces has been suggested by Barton and Bandis (1992). The method is shown in Figure 5.3 and the JRC is estimated from the tilt angle α by means of the following equation.

$$JRC = \frac{\alpha - \phi_b}{\log_{10} \left[\frac{JCS}{\sigma_n} \right]}$$

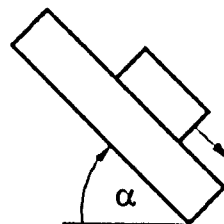


Figure 5.3

For small samples, the normal stress σ_n may be as low as 0.001 MPa. Assuming this value for a typical case in which the tilt angle $\alpha = 65^\circ$, the basic friction angle $\phi_b = 30^\circ$ and the joint wall compressive strength JCS = 100 MPa, gives JRC = 7.

The last of the coefficients that needs to be quantified is the JCS, joint wall compressive strength. Hoek et al (1992) address this calculation and give some guidelines which equate JCS to the uniaxial compressive strength of the rock materials. Table 5.2 summarises this work and Table 5.3 lists peak and residual shear strength of filled discontinuities. Of particular relevance is the Schmidt hammer data.

Table 5.2 Field estimates of joint wall compressive strength (JCS)

Term	Uniaxial Comp. Strength (MPa)	Point Load Index (MPa)	Schmidt hardness (Type L - hammer)	Field estimate of strength	Examples*
Extremely Strong	> 250	>10	50 - 60	Rock material only chipped under repeated hammer blows, rings when hit	Fresh basalt, chert, diabase, gneiss, granite, quartzite
Very strong	100 - 250	4 - 10	40 - 50	Requires many blows of a geological hammer to break intact rock specimens	Amphibolite, sandstone, basalt, gabbro, gneiss, granodiorite, limestone, marble, rhyolite, tuff
Strong	50 - 100	2 - 4	30 - 40	Hand held specimens broken by a single blow of geological hammer	Limestone, marble, phyllite, sandstone, schist, shale
Medium strong	25 - 50	1 - 2	15 - 30	Firm blow with geological pick indents rock to 5 mm, knife just scrapes surface	Claystone, coal, concrete, schist, shale, siltstone
Weak	5 - 25	**	< 15	Knife cuts material but too hard to shape into triaxial specimens	Chalk, rocksalt, potash
Very weak	1 - 5	**		Material crumbles under firm blows of geological pick, can be shaped with knife	Highly weathered or altered rock
Extremely weak	0.25 - 1	**		Indented by thumbnail	Clay gouge

* All rock types exhibit a broad range of uniaxial compressive strengths which reflect the heterogeneity in composition and anisotropy in structure. Strong rocks are characterized by well interlocked crystal fabric and few voids.

** Rocks with a uniaxial compressive strength below 25 MPa are likely to yield highly ambiguous results under point load testing.

A knowledge of the shear strength of filled joints or discontinuities is also important for mine rock engineers concerned with the stability of excavations and Table 5.2 gives some information with respect to peak and residual estimates of cohesion and friction angles. Most of the data has been derived from rocks not normally encountered in South African mines. However, it is significant that quartzitic rocks appear to have the largest values of peak shear strength (31-41 MPa) and peak cohesion (0,6 - 0,7 MPa).

Table 5.3 Shear strength of filled discontinuities and filling material (After Barton, 1974)

Rock	Description	Peak c' (MPa)	Peak φ°	Residual c' (MPa)	Residual φ°
Basalt	Clayey basaltic breccia, wide variation from clay to basalt content	0.24	42		
Bentonite	Bentonite seam in chalk Thin layers Triaxial tests	0.015 0.09-0.12 0.06-0.1	7.5 12-17 9-13		
Bentonitic shale	Triaxial tests Direct shear tests	0-0.27	8.5-29	0.03	8.5
Clays	Over-consolidated, slips, joints and minor shears	0-0.18	12-18.5	0-0.003	10.5-16
Clay shale	Triaxial tests Stratification surfaces	0.06	32	0	19-25
Coal measure rocks	Clay mylonite seams, 10 to 25 mm	0.012	16	0	11-11.5
Dolomite	Altered shale bed, ± 150 mm thick	0.04	14.5	0.02	17
Diorite, granodiorite and porphyry	Clay gouge (2% clay, PI = 17%)	0	26.5		
Granite	Clay filled faults Sandy loam fault filling Tectonic shear zone, schistose and broken granites, disintegrated rock and gouge	0-0.1 0.05 0.24	24-45 40 42		
Greywacke	1-2 mm clay in bedding planes			0	21
Limestone	6 mm clay layer 10-20 mm clay fillings <1 mm clay filling	0.1 0.05-0.2	13-14 17-21	0	13
Limestone, marl and lignites	Interbedded lignite layers Lignite/marl contact	0.08 0.1	38 10		
Limestone	Marlaceous joints, 20 mm thick	0	25	0	15-24
Lignite	Layer between lignite and clay	0.014-.03	15-17.5		
Montmorillonite Bentonite clay	80 mm seams of bentonite (montmorillonite) clay in chalk	0.36 0.016-.02	14 7.5-11.5	0.08	11
Schists, quartzites and siliceous schists	100-15- mm thick clay filling Stratification with thin clay Stratification with thick clay	0.03-0.08 0.61-0.74 0.38	32 41 31		
Slates	Finely laminated and altered	0.05	33		
Quartz / kaolin / pyrolusite	Remoulded triaxial tests	0.042-.09	36-38		

5.2 Rock Mass Rating System (RMR)

Bieniawski (1973) published details of a rock mass classification system or Rock Mass Rating System, which has subsequently been modified and refined. The parameters used to classify the rock mass condition are:

- 1 Uniaxial compressive strength of rock material.
- 2 Rock Quality Designation (RQD).
- 3 Spacing of discontinuities.
- 4 Condition of discontinuities.
- 5 Groundwater conditions.
- 6 Orientation of discontinuities.

In applying this classification system, the rock mass is divided into a number of structural regions and each region is classified separately. The boundaries of the structural regions usually coincide with a major structural feature such as a fault or with a change in rock type. In some cases, significant changes in discontinuity spacing or characteristics, within the same rock type, may necessitate the division of the rock mass into a number of small structural regions.

The Rock Mass Rating system is given in Table 5.2.1 which can be used to rate each of the six parameters listed above. These ratings are summed to give a value of RMR between 0 and 100.

Table 5.2.1 summarizes the system as a whole and in addition, Table 5.2.2 illustrates the application of the system to the selection of tunnel support systems. The system is generally more applicable to civil engineering applications than it is to deep mines. However, Laubscher (1976) and his co-workers Laubscher and Taylor, 1976 and Page and Taylor have modified the system so as to account for the in-situ stress state, induced stress, stress change and the effects of blasting. These modified systems are mainly applicable to block caving operations.

Hoek et al (1994) give an example of the application of the system for the development of a tunnel through wet granitic rock which is cut by a set of joints which dip at 60° and have slightly rough weathered surfaces and are 300 mm apart.

Table 5.2.1 Rock Mass Rating System (After Bieniawski, 1989)

A. CLASSIFICATION PARAMETERS AND THEIR RATINGS									
Parameter		Range of values							
1	Strength of intact rock material	Point-load strength index	>10 MPa	4 - 10 MPa	2 - 4 MPa	1 - 2 MPa	For this low range - uniaxial compressive test is preferred		
		Uniaxial comp. strength	>250 MPa	100 - 250 MPa	50 - 100 MPa	25 - 50 MPa	5 - 25 MPa	1 - 5 MPa	< 1 MPa
		Rating	15	12	7	4	2	1	0
2	Drill core quality RQD		90% - 100%	75% - 90%	50% - 75%	25% - 50%	< 25%		
	Rating		20	17	13	8	3		
3	Spacing of discontinuities		> 2 m	0.6 - 2 . m	200 - 600 mm	60 - 200 mm	< 60 mm		
	Rating		20	15	10	8	5		
4	Condition of discontinuities (See E)		Very rough surfaces Not continuous No separation Unweathered wall rock	Slightly rough surfaces Separation < 1 mm Slightly weathered walls	Slightly rough surfaces Separation < 1 mm Highly weathered walls	Slicksided surfaces or Gouge < 5 mm thick or Separation 1-5 mm Continuous	Soft gouge >5 mm thick or Separation > 5 mm Continuous		
	Rating		30	25	20	10	0		
5	Ground water	Inflow per 10 m tunnel length (l/m)	None	< 10	10 - 25	25 - 125	> 125		
		(Joint water press)/ (Major principal σ)	0	< 0.1	0.1 - 0.2	0.2 - 0.5	> 0.5		
	General conditions		Completely dry	Damp	Wet	Dripping	Flowing		
	Rating		15	10	7	4	0		
B. RATING ADJUSTMENT FOR DISCONTINUITY ORIENTATIONS (See F)									
Strike and dip orientations		Very favourable	Favourable	Fair	Unfavourable	Very Unfavourable			
Ratings	Tunnels *and mines	0	-2	-5	-10	-12			
	Foundations	0	-2	-7	-15	-25			
	Slopes	0	-5	-25	-50				
C. ROCK MASS CLASSES DETERMINED FROM TOTAL RATINGS									
Rating	100 ← 81	80 ← 61	60 ← 41	40 ← 21	< 21				
Class number	I	II	III	IV	V				
Description	Very good rock	Good rock	Fair rock	Poor rock	Very poor rock				
D. MEANING OF ROCK CLASSES									
Class number	I	II	III	IV	V				
Average stand-up time	20 yrs for 15 m span	1 year for 10 m span	1 week for 5 m span	10 hrs for 2.5 m span	30 min for 1 m span				
Cohesion of rock mass (kPa)	> 400	300 - 400	200 - 300	100 - 200	< 100				
Friction angle of rock mass (deg)	> 45	35 - 45	25 - 35	15 - 25	< 15				
E. GUIDELINES FOR CLASSIFICATION OF DISCONTINUITY CONDITIONS*									
Discontinuity length (persistence)	< 1 m	1 - 3 m	3 - 10 m	10 - 20 m	> 20 m				
Rating	6	4	2	1	0				
Separation (aperture)	None	< 0.1 mm	0.1 - 1.0 mm	1 - 5 mm	> 5 mm				
Rating	6	5	4	1	0				
Roughness	Very rough	Rough	Slightly rough	Smooth	Slicksided				
Rating	6	5	3	1	0				
Infilling (gouge)	None	Hard filling < 5 mm	Hard filling > 5 mm	Soft filling < 5 mm	Soft filling > 5 mm				
Rating	6	4	2	2	0				
Weathering	Unweathered	Slightly weathered	Moderately weathrd	Highly weathered	Decomposed				
Ratings	6	5	3	1	0				
F. EFFECT OF DISCONTINUITY STRIKE AND DIP ORIENTATION IN TUNNELLING**									
Strike perpendicular to tunnel axis				Strike parallel to tunnel axis					
Drive with dip - Dip 45 - 90°		Drive with dip - Dip 20 - 45°		Dip 45 - 90°		Dip 20 - 45°			
Very favourable		Favourable		Very favourable		Fair			
Drive against dip - Dip 45-90°		Drive against dip - Dip 20-45°		Dip 0-20 - Irrespective of strike°					
Fair		Unfavourable		Fair					

* Some conditions are mutually exclusive . For example, if infilling is present, the roughness of the surface will be overshadowed by the influence of the gouge. In such cases use A.4 directly.

** Modified after Wickham et al (1972).

The RMR value is determined as follows:

Table	Item	Value	Rating
A.1	Point load index	8 MPa	12
A.2	RQD	70%	13
A.3	Spacing of discontinuities	300 m	10
A.4	Condition of discontinuities	Note 1	22
A.5	Groundwater	Wet	7
B	Adjustment for joint orientation	Note 2	-5
		Total	59

Note 1: For slightly rough and altered discontinuity surfaces with a separation of < 1 mm, Table 5.2.1.4 gives a rating of 25. When more detailed information is available, Table 4:E can be used to obtain a more refined rating. In this case the rating would be the sum of 4(1-3 m discontinuity length), 4(separation 0.1-1.0 mm), 3(slightly rough), 6(no infilling) and 5 (slightly weathered) = 22.

Note 2: Table 5.2.1 gives a description of "Fair" for the conditions assumed where the tunnel is to be driven against the dip of a set of joints dipping at 60°. Applying this data to section B "Tunnels and Mines" in Table 5.2.1 gives an adjustment rating of -5.

The value of RMR of 59 indicates that the rock mass is on the boundary between the Fair rock and Good rock classification categories. In the initial stages of design and construction, it is advisable to utilize the support suggested for fair rock. However, if the rock mass surrounding the excavation is expected to undergo large mining induced stress changes, then more substantial support appropriate for the fair rock should be installed. This example indicates good deal of judgement is needed in the application of rock mass classification to support design.

Table 5.2.2 Guidelines for excavation and support of 10 m span rock tunnels in accordance with the RMR system (After Bieniawski (1989)).

Rock mass class	Excavation	Rock bolts (20 mm dia. fully grouted)	Shotcrete	Steel sets
I - Very good rock RMR: 81-100	Full face 3 m advance	Generally no support required except spot bolting		
II - Good rock RMR: 61-80	Full face 1-1.5 m advance Complete support 20 m from face	Locally, bolts in crown 3 m long, spaced 2.5 m with occasional wire mesh	50 mm in crown where required	None
III - Fair rock RMR: 41-60	Top heading and bench 1.5-3 m advance in top heading Commence support after each blast Complete support 10 m from face	Systematic bolts 4 m long, spaced 1.5 - 2 m in crown and walls with wire mesh in crown	50-100 mm in crown and 30 mm in sides	None
IV - Poor rock RMR: 21-40	Top heading and bench 1.0-1.5 m advance in top heading. Install support concurrently with excavation, 10 m from face	Systematic bolts 4-5 m long, spaced 1-1.5 m in crown and walls with wire mesh	100-150 mm in crown and 100 mm in sides	Light to medium ribs spaced 1.5 m where required
V - Very poor rock RMR: < 20	Multiple drifts 0.5-1.5 m advance in top heading. Install support concurrently with excavation. Shotcrete as soon as possible after blasting	Systematic bolts 5-6 m long, spaced 1-1.5 m in crown and walls with wire mesh. Bolt invert	150-200 mm in crown, 150 mm in sides, and 50 mm on face	Medium to heavy ribs spaced 0.75 m with steel lagging and forepoling if required. Close invert

Estimation of in-situ deformation modulus

Hoek et al (1994) reported on a method based on early work by Bieniawski (1978) for determining the in-situ deformation of the rockmass from in-situ RMR values, using the following relationship.

$$E_m = 2 \text{ RMR} - 100$$

where E_m is the in-situ deformation modulus.

An alternative form is:

$$EM = 10 (\text{RMR}-10)/40 \quad (\text{Serafim and Pereira 1983})$$

while Barton (1987) and his co-workers (Barton et al 1992) have found good agreement between measured displacements and predictions from numerical models using $E_m = 25 \log_{10} Q$

Of these equations, that of Serafim and Pereira provides the most reasonable fit with in-situ observations.

6 PROCEDURES FOR DETERMINING THE STIFFNESS AND OTHER PROPERTIES OF JOINTS

Laboratory methods for determining rock deformation or frictional properties include direct shear tests, triaxial tests, shear box tests, double shear tests, where one block of rock is pushed under load, past two retaining blocks of the same material, and rotation tests, where two hollow cylinders are placed together under an axial force N and a torque M is applied to rotate the two cylinders past each other. This test allows for large amounts of sliding, and lastly the use of extension and shear fracture surfaces, produced under load in the laboratory.

Jaeger (1971) outlines the important aspects of rock friction with respect to rock mechanics applications. These include available methods for measuring friction, the effect of gouge generation on the sliding surfaces, which appears to be time-dependent, and the need for more precise measurements of friction.

With respect to the determination of joint friction, Byerlee (1977) has shown that at high pressures; i.e. pressures in excess of 200 MPa, the friction coefficient is independent of rock type, pressure, surface roughness etc., and can be described by a straight line.

$$\tau = 0,5 + 0,6 \sigma_n$$

At lower pressures i.e. 0 - 100 MPa, a similar linear relationship exists, namely

$$\tau = 0,85 \sigma_n$$

although the scatter is much greater.

Rosso (1976) discussed the application of other test methods to determine values of shear and normal stiffness determined in direct shear tests and jointed triaxial tests and compared these to in-situ measurements by Pratt et al (1972). The table below summarises these results

DIRECT SHEAR		JOINTED TRIAXIAL		IN-SITU	
σ_n (MPa)	K_s (MPa/cm)	σ_n (MPa)	K_s (MPa/cm)	σ_n (MPa)	K_s (MPa/cm)
3,5	$0,43 \pm 5$	1-3	$0,2 \pm 0,1$	0-1,2	0,16
7,0	$0,5 \pm 5$	3,5-8,5	$0,3 \pm 0,15$	0-2,8	0,12
10,5	$0,8 \pm 5$	7-18	$0,9 \pm 0,5$	0-6,3	$0,48 \pm 2$

Other work which is relevant to estimates of joint stiffness is that of Stimpson and Chen (1993) who used a bimodal compression and tension device to evaluate stiffness moduli in both tension and compression. Large differences in the magnitude of the Young's moduli for a granite and a limestone were noted with the ratio of the modulus in tension and compression varying from $E_t/E_c = 1$ to $E_t/E_c = 0,3$ for the rock types tested.

Bimodular behaviour is of significance in situations where tensile and/or uniaxial tensile/compressive stresses are encountered, such as hangingwall beams, ore passes, boreholes and areas where mixed compression - tension forces are encountered.

Also of significance with respect to the degradation of shear surfaces is the work on shear failure mechanisms of profiled surfaces by Roberds et al (1978) and by Pereira and de Freitas (1993) using a direct shear test apparatus. For this work profiled surfaces, artificially

prepared from joint surfaces in natural sandstone, were used. The testing procedure was to apply a normal stress followed by a shear stress. Several stages of degradation were noted, namely: static friction, mobilisation of the initial shear stiffness, sliding, brittle fracture and post-peak failure of the asperity surfaces. For large displacements the gouge material is progressively crushed, resulting in a reduction in grain size, enhancing the potential for sudden slip.

This scenario is relevant not only to failure or slip on natural discontinuities but also to inclined stress induced fractures in deep mine stopes. Values of some of the parameters used for the modelling work were JRC: 0 - smooth and > 20 -rough; JCS : = UCS of rock type for low normal stress, to peak triaxial strength for high σ_n .

The peak dilation rate or non-associated flow rule, for a rock discontinuity and coefficient of friction ϕ was determined experimentally, to be

$$\left[\frac{\delta_{\epsilon} \text{ normal}}{\delta_{\epsilon} \text{ shear}} \right] = \tan \left[\frac{JRC}{2} \log \left(\frac{JCS}{\sigma_n} \right) \right] \quad - \text{(eq.13)}$$

Roberds and Einstein (1978) also evaluated the Goodman (1974) model which was developed to quantify observations made in direct shear tests on rock discontinuities, for application to finite element models.

7 CONCLUSIONS

The adequate representation of joint behaviour is a very important aspect of the analysis of most rock engineering problems. A great variety of joint models have been proposed but only a few of these are used in practice in the SA mining industry. Each model has limitations. The choice of model is of prime importance, only once this choice has been made does the question of parameter values arise. The determination of suitable parameters for a given model requires interpretation of experimental data with specific reference to the model. Joint models are applied in numerical models of engineering problems, some adjustment of joint model parameters, from those indicated by experimental data, is often made to compensate for simplification of joint geometry and other aspects of the problem. This aspect of the application of joint models makes it particularly difficult to provide guide lines for parameter values since adjustments are problem specific.

Study of the literature has revealed that there are many aspects of joint behaviour that can be taken into account. Several key aspects of joint behaviour have been identified, these include:

- 1) the peak shear strength of a joint.
- 2) the change in shear resistance with continuing shear displacement on a joint.
- 3) the dilation that occurs with shear displacement on a joint.
- 4) the effects of shear reversal on joint behaviour.

Other issues seem to be of lesser importance, particularly in the context of application to typical rock engineering problems.

Of the key issues, the effect of shear reversals is the one that is not adequately accounted for with joint models currently in use. The assessment suitable values for parameters governing dilation in existing models is particularly difficult even in the absence of shear reversals. Changes in shear resistance often require good assessment of the in situ condition of joints, particularly where previous movements have taken place on these joints. In many instances where only the peak shear strength of joints is required a simple Coulomb criterion is adequate, but it is noted that the value of the cohesion used is of great significance. The presence of rock bridges is an issue that has significant impact on peak strength calculations in some circumstances.

ACKNOWLEDGEMENT

Permission from Evert Hoek to quote from Chapters 4 and 5 of the book "Design of Support for Underground Hardrock Mines" is gratefully acknowledged.

REFERENCES

Archambault G, Fortin M, Gill D.E, Aubertin M, and Ladanyi, B. Experimental investigations for an algorithm simulating the effect of variable normal stiffness on discontinuities shear strength. Rock Joints : Proceedings of the international symposium on rock joints, Norway. (eds. N. Barton, and O Stephansson). Balkema, Rotterdam, (1990). p. 141-148.

Amadel B, and Saeb. Constitutive models for rock joints. Rock Joints : Proceedings of the international symposium on rock joints, Norway. (eds. N. Barton, and O Stephansson). Balkema, Rotterdam, (1990). p. 481 - 594.

Aydan Ö, Khikwa Y, Ebisu S, Komura S, and Watanabe A. Studies on interfaces and discontinuities and an incremental elasto-plastic constitutive law. *Rock Joints : Proceedings of the international symposium on rock joints, Norway.* (eds. N. Barton, and O Stephansson). Balkema, Rotterdam, (1990).

Bandis S C. Scale effects in the strength and deformability of rocks and rock joints. *Proceedings of the first international workshop on scale effects in rock masses, Norway.* (ed. A Pinto da Cunha). Balkema, Rotterdam, (1990a). p. 59-76.

Bandis S C. Mechanical properties of rock joints. *Rock Joints : Proceedings of the international symposium on rock joints, Norway.* (eds. N. Barton, and O Stephansson). Balkema, Rotterdam, (1990b). p. 125-140.

Barton N.R. *Rock Mechanics Review - The shear strength of rock and rock joints.* *Int. Journal, Rock Mechanics Min. Sci. and Geomech. Abstr.* V.13, pp. 255-279 (1976).

Barton N.R., Lien R., and Lunde J. (1974) Engineering classification of rock masses for the design of tunnel support. *Rock Mech*, V.6, 189-239.

Barton N.R., and Bandis S.C. (1990) Review of predictive capabilities of JRC - JCS model in engineering practise. *Rock Joints, Barton and Stephansson (eds.)*, 1 Balkema, Rotterdam.

Barton N.R., and Choubey V. The shear strength of rock joints in theory and practice. *Rock Mechanics* (1977), p. 1-54

Barton N.R., Bandis S., and Bakhtar, K. Strength, deformation and conductivity coupling of rock joints, *Int. Rock Mech. Min. Sci. Geomech. Abstr.* V.22, pp 121-140 (1985).

Barton N.R. Scale effect on sampling bias *Scale effects in rock masses, Pinta da Cunha (ed)* Balkema, Rotterdam, pp. 31-55 (1990).

Barton N.R., and Bakhtar K. Rock joint description and modelling for the hydrothermal mechanical design of nuclear waste repositories. *TerraTek Engineering; TRE 83-10 parts 1-4*, pp 270 (1983).

Benjelloun Z H, Boulon and Billaux D. Experimental and numerical investigations of rock joints. *Rock Joints : Proceedings of the international symposium on rock joints, Norway.* (eds. N. Barton, and O Stephansson). Balkema, Rotterdam, (1990). p. 171-178.

Bieniaswski Z.T. Determining rock mass deformability - experiences from case histories. *Int. J. Rock Mech. Min. Sci. Geomech Abstr.* Vol. 15, 237-247 (1978).

Bieniaswski Z.T. *Rock Mechanics design in mining and tunnelling*, pp 97-133, Rotterdam A.A Balkema (1989).

Blandford M L, Key S W, and Chieslar JD. A general 3-D model for a jointed rock mass constitute laws for engineering materials : Theory and applications. (ed. Desai et al) Elsevier (1987).

Blandford M L, and Key S W. An example of continuum versus quasi-discrete modelling of a jointed rock mass. In *Constitutive Laws for Engineering Materials: Theory and Applications* (ed. C.S. Desai et al) Elsevier. (1987).

Blqiwias T E, and Hansen F D. Scale effects in the shear behaviour of joints in welded tuff. *Rock Joints : Proceedings of the international symposium on rock joints, Norway.* (eds. N. Barton, and O Stephansson). Balkema, Rotterdam, (1990). p. 185-189.

Brady B H G, and Brown E T. *Rock Mechanics for underground mining.* George, Allen and Unwin, Londen, (1985).

Bro A. Stick-slip behaviour of smooth joints (a technical note). *International Journal of Rock Mechanics, Mining Sciences and Geomechanics Abstracts.* Vol. 29. (1992b). p. 171-177.

Bro A. Failure of stepped joints: an analysis and comparison with measured failure geometry (a technical note). *International Journal of Rock Mechanics, Mining Sciences and Geomechanics Abstracts.* Vol. 29. (1992c). p. 179-186.

Chryssanthakis P, and Barton N. Joint roughness (JRC_n) characterization of a rock joint and joint replica at 1 m scale. *Rock Joints : Proceedings of the international symposium on rock joints, Norway.* (eds. N. Barton, and O Stephansson). Balkema, Rotterdam, (1990). p. 27-33.

Cuislat F D E, Hyett A J, and Hudson J A. Numerical investigation of the boundary conditions effect on rock joint behaviour. *Rock Joints : Proceedings of the international symposium on rock joints, Norway.* (eds. N. Barton, and O Stephansson). Balkema, Rotterdam, (1990). p. 611-616.

Cundall P A., and Lemos (1990). Numerical simulation of fault instabilities with a continuously yielding joint model. Proceedings of the 2nd International Symposium on Rockbursts and Seismicity in Mines. Balkema Rotterdam (1990), pp. 147-153.

Desai C S, and Fishman K L. Plasticity-based constitutive model with associated testing for joints. International Journal of Rock Mechanics, Mining Science and Geomechanics Abstracts. Vol. 28. (1991). p. 15-29.

Desai C S, and Youzhi M. Modelling of joints and interfaces using the disturbed-state concept. International Journal for Numerical and Analytical Methods in Geomechanics. Vol. 16. (1992). p. 623-653.

Fishman Y.A. Failure mechanism and shear strength of joint wall asperities. Rock Joints : Proceedings of the international symposium on rock joints, Norway. (eds. N. Barton, and O Stephansson). Balkema, Rotterdam, (1990). p. 627-631.

FLAC Ver. 3.2 User Manual, ITASCA (1992).

Goodman R.E. The mechanical properties of joints. Proc. 3rd Congr. Int. Soc. for rock Mechanics. Denver Colorado, Vol. 1A pp. 122-140 (1974).

Hoek E, Kaiser P K, and Bawden W F. Design of support for underground hard rock mines. Book manuscript 1993 (to be published 1994).

Hoek E, and Brown E T. Underground excavations in rock. Stephen Austin, Hertford England, 1982.

Hsiung S, Ghash A, and Chowdhury A H. An investigation of rock joint models on prediction of joint behaviour under pseudostatic cyclic shear loads. Rock Mechanics: Models and Measurements, Challenges from Industry. The proceedings of the 1st Northern American Rock Mechanics Symposium, Austin, Texas. (eds. P.P. Nelson and S.E. Laubach). Balkema, Rotterdam, (1994). p. 111-119.

Huang T H, and Doong Y S. Anisotropic shear strength of rock joints. Rock Joints : Proceedings of the international symposium on rock joints, Norway. (eds. N. Barton, and O Stephansson). Balkema, Rotterdam, (1990). p. 211-218.

- Huang X, Haimson B C, Plesha M E, and Qui X. An investigation of the mechanics of rock joints. Part I : Laboratory Investigation. *International Journal of Rock Mechanics, Mineral Science and Geomechanics Abstracts*. Vol. 30. (1993). p. 257-269.
- Hutson R W, and Dowding C H. Joint asperity degradation during cyclic shear. *International Journal of Rock Mechanics, Mining Sciences and Geomechanics Abstracts*. Vol. 27. (1990). p. 109-119.
- Jing L. A two dimensional constitutive model of rock joints with pre- and post-peak behaviour. *Rock Joints : Proceedings of the international symposium on rock joints, Norway*. (eds. N. Barton, and O Stephansson). Balkema, Rotterdam, (1990). p. 637-638.
- Jing L, Stephansson O, and Nordlund E. Study of rock joints under cyclic loading conditons. *Rock Mechanics*, Vol. 26. (1993), p. 215-232.
- Kane W F, and Drumm E C. A modified 'cap' model for rock joints. *Proceedings of the 28th Symposium on Rock Mechanics*. Tuscon. (1987).
- Kazakids V N, and Diedrichs M S. Understanding jointed rock mass behaviour using ubiquitous joint approach. *International Journal of Rock Mechanics, Mining Sciences and Geomechanics Abstracts* Vol. 30, p. 163-172 (1993).
- Ke T C, and Goodman R E. Discontinuous deformation analysis and 'the artificial joint concept'. *Rock Mechanics: Models and Measurements, Challenges from Industry*. The proceedings of the 1st Northern American Rock Mechanics Symposium, Austin, Texas. (eds. P.P. Nelson and S.E. Laubach). Balkema, Rotterdam, (1994). p. 599-606.
- Kulatiluke, P H S W, Wathugala D N, and Stephansson O. Joint network modelling, including a validation to an area in Stripa mine, Sweden. *International Journal of Rock Mechanics and Mining Sciences* (in press).
- Kutter H K, and Otto F. Influence of parallel and cross joints on shear behaviour of rock discontinuities. *Rock Joints : Proceedings of the international symposium on rock joints, Norway*. (eds. N. Barton, and O Stephansson). Balkema, Rotterdam, (1990). p. 243-250.

Ladanyi B. and Archambault G. Simulation of shear behaviour of a jointed rock mass. *Rock Mechanics: theory and practice. Proc. 11th U.S. Rock Symposium on rock mechanics. W.H. Somerton (ed), AIME, New York (19..), pp. 105-125.*

Lee M.F. Shear mechanics of bedding phases at Mount Isa Mines, Queensland Melbourne 10-15 May 1983, *Proc 5th ISRM Congress; Workshops on Joints.*

Li C, Stephansson O, and Savilahti T. Behaviour of rock joints and rock bridges in shear testing. *Rock Joints : Proceedings of the international symposium on rock joints, Norway. (eds. N. Barton, and O Stephansson). Balkema, Rotterdam, (1990). p. 259, 266.*

Lorig L V, and Hobbs B E. Numerical modelling of slip instability using the distinct element method with state variable friction laws. *International Journal of Rock Mechanics, Mining Sciences and Geomechanics Abstracts. Vol. 27. (1990). p. 525-534.*

Makarot, A., Barton, N., Vik, G., Chryssanthakis, P., and Monsen, K. Jointed rock mass modelling. *Rock Joints : Proceedings of the international symposium on rock joints, Norway. (eds. N. Barton, and O Stephansson). Balkema, Rotterdam, (1990). p. 647-656.*

Moore D E, Summers R, and Byerlee JD. Relationship between textures and sliding motion of experimentally deformed fault gauge : Application to fault zone behaviour. *Key Questions in Rock Mechanics : Proceedings of the 29th US Symposium, Minneapolis. (eds. P.A. Cundall, R.L. Sterling and A.M. Starfield), Balkema, Rotterdam, (1988). p. 103-110.*

Muralha J, and Pinto da Cunha A. About LNEC experience on scale effects in the mechanical behaviour of joints. *Proceedings of the first international workshop on scale effects in rock masses, Norway. (ed. A Pinto da Cunha). Balkema, Rotterdam, (1990). p. 131-148.*

Muralha J. Evaluation of mechanical characteristics of rock joints under shear loads. *Rock Joints : Proceedings of the international symposium on rock joints, Norway. (eds. N. Barton, and O Stephansson). Balkema, Rotterdam, (1990). p. 657-666.*

Muralha J, and Pinto da Cunha A. Analysis of scale effects in joint mechanical behaviour. *Proceedings of the first international workshop on scale effects in rock masses, Norway. (ed. A Pinto da Cunha). Balkema, Rotterdam, (1990). p. 191-200.*

Napier J A L, and Hildyard M W. Simulation of fracture growth around openings in highly stressed brittle rock. *SAIMM Journal* V.92 (6) 1992, p 159-168.

Ohmishi Y, and Dharmaratne P G R. Shear behaviour of physical models of rock joints under constant normal stiffness conditions. *Rock Joints : Proceedings of the international symposium on rock joints, Norway.* (eds. N. Barton, and O Stephansson). Balkema, Rotterdam, (1990). p. 267, 273.

Olson J, and Pollard D D. Inferring stress from detailed joint geometry. *Key Questions in Rock Mechanics : Proceedings of the 29th US Symposium, Minneapolis.* (eds. P.A. Cundall, R.L. Sterling and A.M. Starfield), Balkema, Rotterdam, (1988). p. 159-167.

Olsson W A. The effects of normal stress history on rock friction. *Key Questions in Rock Mechanics : Proceedings of the 29th US Symposium, Minneapolis.* (eds. P.A. Cundall, R.L. Sterling and A.M. Starfield), Balkema, Rotterdam, (1988). p. 111-117.

Owen D.R.J., Munjiza, A., and Bicanic. A finite element - discrete element approach to the simulation of rock blasting problems. *Proceedings FEMSA-92, 11th Symposium on Finite element Methods in South Africa.* Cape Town (1992) pp. 39-59.

Papaliangas T, Lumsden A C, Henchler S R, and Manolopoulos S. Shear strength of modeled filled rock joints. *Rock Joints : Proceedings of the international symposium on rock joints, Norway.* (eds. N. Barton, and O Stephansson). Balkema, Rotterdam, (1990). p. 275, 282.

Patton F.D. Multiple modes of shear failure in rock . *Proc. Intl. Cong. Rock Mech.* Lisbon, pp. 509-513 (1966).

Pereira J P. Shear strength of filled discontinuities. *Rock Joints : Proceedings of the international symposium on rock joints, Norway.* (eds. N. Barton, and O Stephansson). Balkema, Rotterdam, (1990). p. 283, 287.

Pereira J.P. and de Freitas M.H. Mechanisms of shear failure in artificial fractures of sandstone and their implications for models of hydromechanical coupling. *Rock Mech. Rock Eng.* V. 26, pp. 195-214.

Phien-Wej N, Shrestha U B, and Rantucci G. Effect of infill thickness on shear behaviour of rock joints. *Rock Joints : Proceedings of the international symposium on rock joints, Norway.* (eds. N. Barton, and O Stephansson). Balkema, Rotterdam, (1990). p. 289, 294.

Pande G N, Beer G, and Williams J R. Numerical methods in rock mechanics. Wiley, Chichester. (1990).

Plesha M.E. Constitutive models for rock discontinuities with dilatancy and surface degradation. Int. J. Numerical Mod. Methods Geomech. V.11, pp. 345-362 (1987).

Plesha M E, Hutson W R, and Dowding C H. Determination of asperity damage parameters for constitutive models of rock discontinuities. International Journal for Numerical Methods in Geomechanics, Vol. 15. (1991). p. 289-294.

Plesha M.E. and Haimson B.C. An advanced model for rock joint behaviour: analytical, experimental and implementational considerations. Proc. 29th U.S. Symposium on Key Questions in Rock Mechnancis. pp. 119-126 (1988).

Price N J. Fault and development in brittle and semi-brittle rock. Pergamon Oxford. (1966).

Pollard D, and Aydin 1988. Progress in understanding jointing over the past century. Geol. Soc. AM Bulletin V. 100, p 1181-1204. (1988)

Qui X, Plesha M E, Haung X, and Haimson B C. An investigation of the mechanics of rock joints. Part II : Analytical Investigation. International Journal of Rock Méchanics, Mineral Science and Geomechanics Abstracts. Vol. 30. (1993). p. 271-287.

Roberds W I and Einstein H M. (1978) Comprehensive model of rock discontinuities; Jnl. Goetechnical Engineering Div. Proc. ASCE VOI. 104, No. GT5, May, p 553-569.

Roko R O, and Daemen J J K. Analysis of deformation of joint asperities and mechanical implications. Key Questions in Rock Mechanics : Proceedings of the 29th US Symposium, Minneapolis. (eds. P.A. Cundall, R.L. Sterling and A.M. Starfield), Balkema, Rotterdam, (1988). p. 127-134.

Sage J D, Aziz A A, and Denek E R. Aspects of scale effects on rock closure. Proceedings of the first international workshop on scale effects in rock masses, Norway. (ed. A Pinto da Cunha). Balkema, Rotterdam, (1990). p. 175-181.

- Savilahti T, Nordlund E, and Stephansson O. Shear box testing and modelling of joint bridges. *Rock Joints : Proceedings of the international symposium on rock joints, Norway.* (eds. N. Barton, and O Stephansson). Balkema, Rotterdam, (1990). p. 295-299.
- Scholz C H. *The mechanics of earthquakes and faulting.* Cambridge University Press, Cambridge, 1990.
- Skinas C A, Bandis S C, and Deminis C A. Experimental investigations and modelling of rock joint behaviour under constant stiffness. *Rock Joints : Proceedings of the international symposium on rock joints, Norway.* (eds. N. Barton, and O Stephansson). Balkema, Rotterdam, (1990). p. 301-308.
- Stimpson B. and Chen R. Measurement of rock elastic moduli in tension and in compression and its practical significance. *Canadian Geotechnical Journal* V.30, pp. 338-347, (1993).
- Snyman M F. Numerical modelling of dilatant rock joints. Ph.D. dissertation. University of Cape Town, South Africa. (1991).
- ITASCA. UDEC. Universal distinct element code. Ver. ICG 2.0 User manual, ITASCA Consulting Group Inc. Minneapolis, Minnesota, USA (1993).
- Xainbin Y, and Vayssade B. Joint profiles and their roughness parameters (technical note). *International Journal of Rock Mechanics, Mineral Science and Geomechanics Abstracts.* Vol. 28. (1991). p. 333-336.

APPENDIX 1 : SUMMARY OF ROCK DEFORMATION AND OTHER PROPERTIES

IN-SITU MEASUREMENTS

MOUNT ISA MINE (Lee 1983)

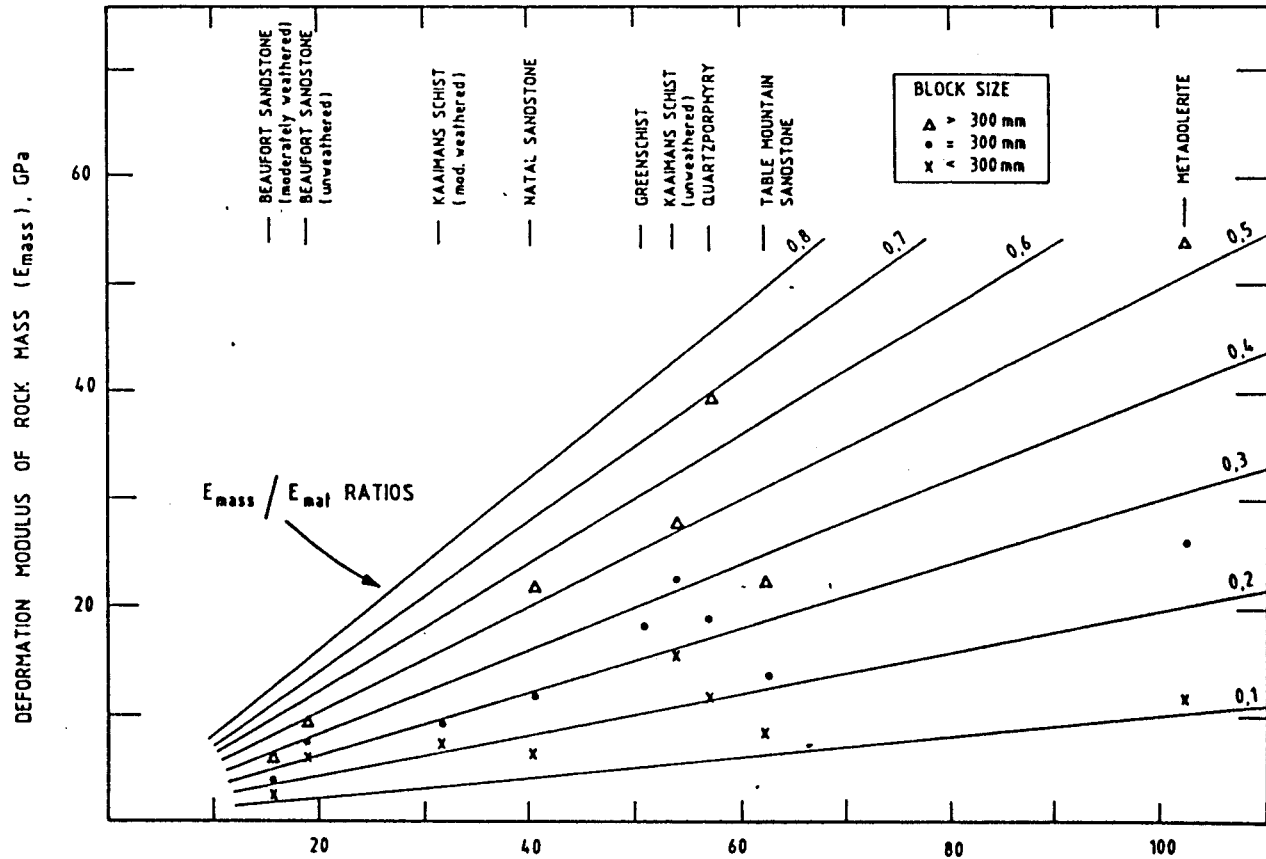
- 1 Asperity angle i_1 : $\sigma_N > 50 \text{ MPa}$ $i_1 = 2,5^\circ$ $\phi = 11^\circ$
 $\sigma_N \sim 2 \text{ MPa}$ $i_1 = 12^\circ$ $\phi = 20,5^\circ$
- 2 JRC : 12
- 3 Angle of sliding friction : ϕ_u 8,5°
- 4 Typical weak Mount Isa bedding plane shear stiffness values (MPa/m)

L (m)	σ_N (MPa)	100	60	0
	Situation - mining Geological	Cut-and-fill stope crown pillar	Sublevel open stope transverse pillar	Hangingwall or footwall of stopes
0.2	Hangingwall 11, 13/80 orebody, footwall 9 orebody Bedding plane spacing $\approx 0.1 \text{ m}$	8 565	5 460	0
2	Hangingwall 6, 7 or 8 orebody Bedding plane spacing $\approx 6 \text{ m}$	857	546	0
5	Within orebodies Bedding plane spacing $\approx 5 \text{ m}$	343	218	0

L = joint length.

APPENDIX 1 CONTINUED : RELATIONSHIP BETWEEN ROCK MASS AND ROCK MATERIAL IN-SITU MODULI (Schall and Vogler, 1988)

Test methods: Good man jack tests in NX boreholes; plate jacking tests.

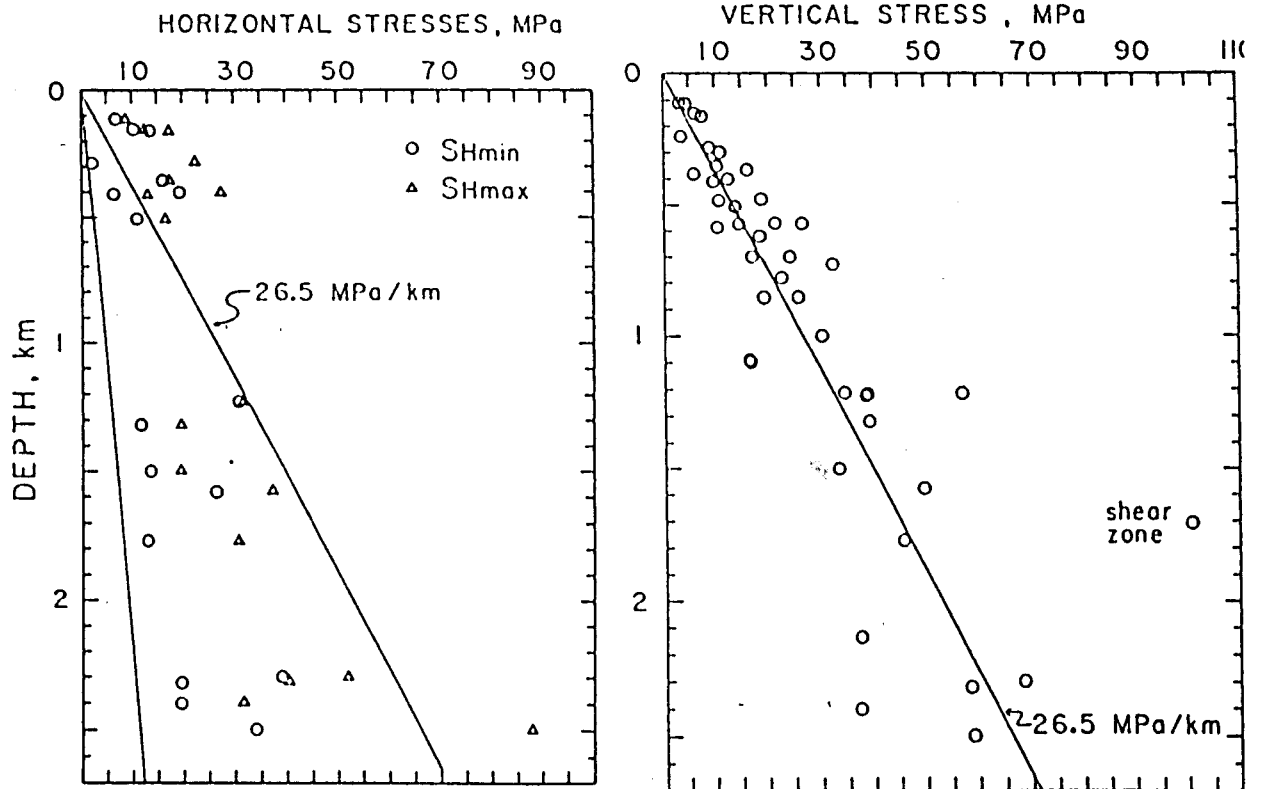


Deformation modulus of rock material (E_{mat}), GPa
Relationship between block size and E_{mass} / E_{mat} ratio

TABLE 1 In-situ stress measurements in Southern Africa (McGarr and Gay, 1987)

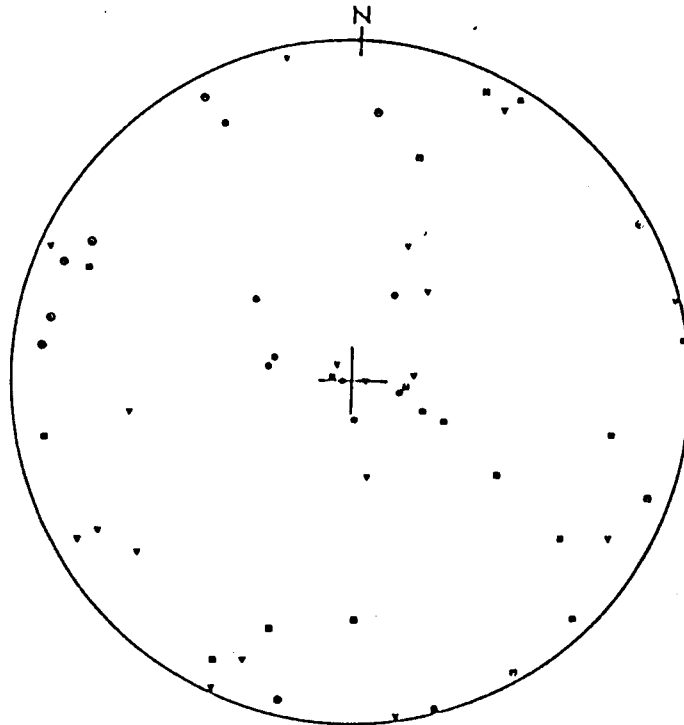
Locality	Depth m	S_1 MPa	Azimuth Degrees	Plunge Degrees	S_2 MPa	Azimuth Degrees	Plunge Degrees	S_3 MPa	Azimuth Degrees	Plunge Degrees
Roodepoort, Transvaal, SA	2 500	88.0	332	18	58.0	112	67	34.0	238	15
Boksburg, Transvaal	2 400	40.3	024	67	31.5	136	9	19.5	230	21
Carletonville, Transvaal	2 320	62.5	285	70	40.5	030	5	19.5	120	15
Roodepoort, Transvaal	2 300	70.0	112	72	52.0	292	18	39.0	203	1
Carletonville, Transvaal	1 770	55.2	280	70	30.6	126	26	13.0	028	11
Evander, Transvaal	1 577	49.5	270	88	37.2	081	2	26.4	171	1
Virginia, Orange Free State	1 500	33.5	176	81	19.3	024	8	13.5	294	4
Carletonville, Transvaal	1 320	46.0	310	60	19.5	100	25	11.5	200	15
Evander, Transvaal	1 226	38.6	100	79	31.2	257	10	31.0	345	5
Evander, Transvaal	508	16.5	164	2	13.9	284	85	11.0	074	5
Copperton, Cape Province	410	13.0	330	6	9.6	098	78	6.4	239	6
Copperton, Cape Province	279	22.4	004	22	8.8	123	48	2.5	260	33
Drakensburg, Natal	150	12.4	297	13	10.2	206	8	5.9	086	75
Drakensburg, Natal	111	8.7	060	3	6.8	150	2	3.0	090	87
Ruacana, South West Africa	115	8.8	192	3	6.9	111	7	3.9	308	83
Shabani, Zimbabwe	350	17.3	279	13	16.1	013	33	8.4	170	57
Kafue Gorge, Zambia	160	17.3	291	10	13.7	197	26	7.1	039	62
Kafue Gorge, Zambia	400	27.5	275	10	19.4	177	32	12.2	021	55

IN-SITU STRESS RESULTS



Horizontal stresses measured in Southern Africa

Vertical component of stress for depths greater than 100 m.



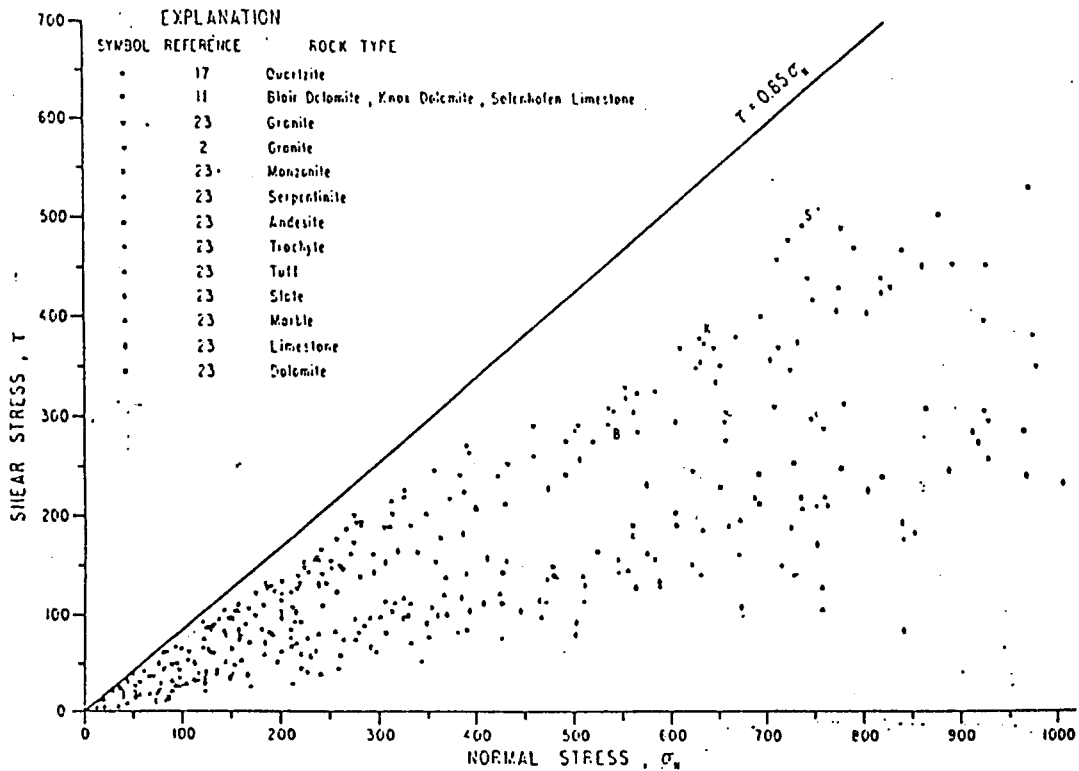
Orientation of principal stresses measured in Southern Africa after Gay (1975, 1977) and Van Heerden (1976). filled symbols refer to sites within the Witwatersrand system and open symbols to sites elsewhere. Circles denote S_1 , squares S_2 , triangles S_3 . this is an equal area projection of the lower hemisphere.

LABORATORY TESTING

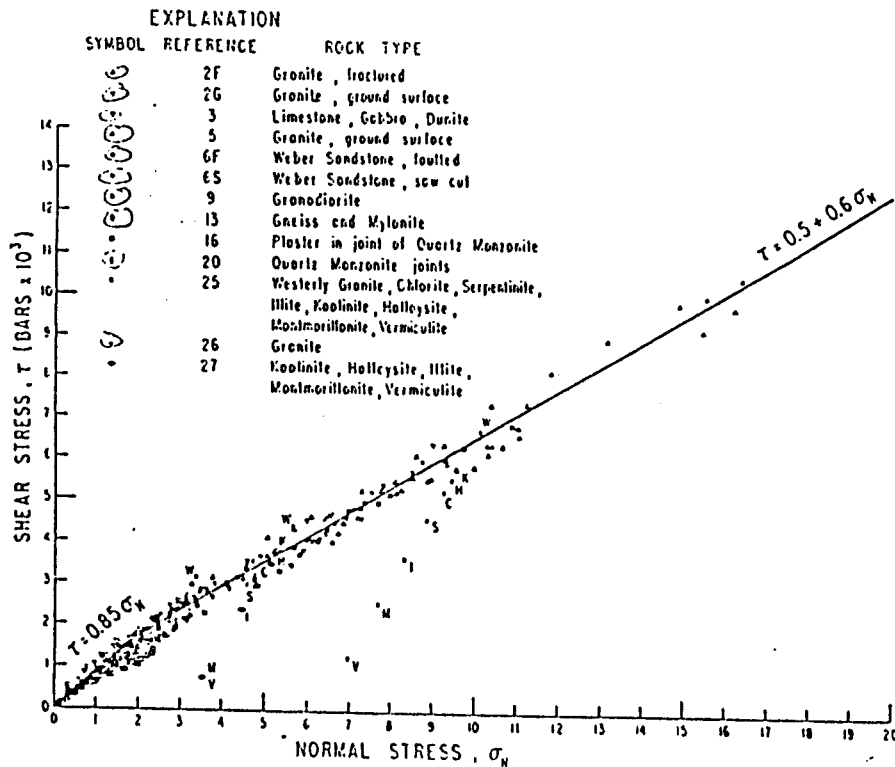
1 Byerlee (1978) : Laboratory test results for various rock types.

Shear Stress	Normal Stress	Coefficient of Friction
0 - 20 MPa 20 - 200	0 - 20 MPa 20 - 200	$\tau = 0,85 \sigma_n$ $\tau = 0,5 + 0,60 \sigma_n$

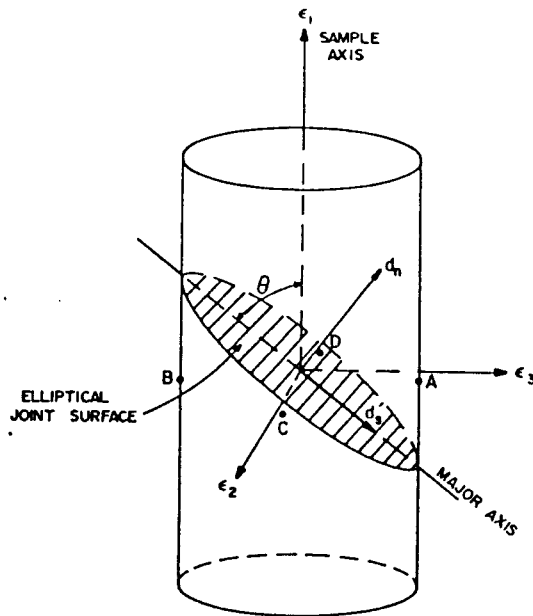
FRICITION MEASURED AT YIELD STRESS



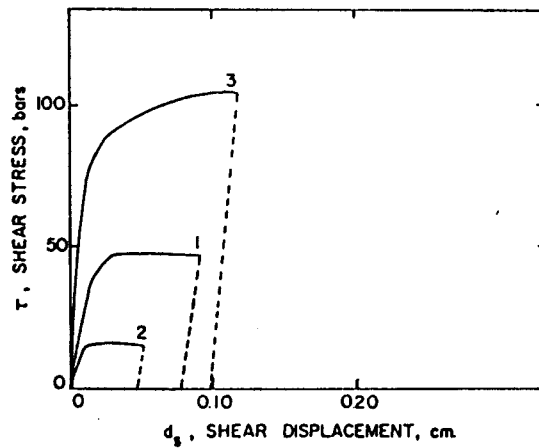
FRICITION MEASURED AT MAXIMUM, STRESS



2 Rosso (1976) : Jointed triaxial test



Jointed triaxial specimen showing joint plane, strain, and displacement orientations



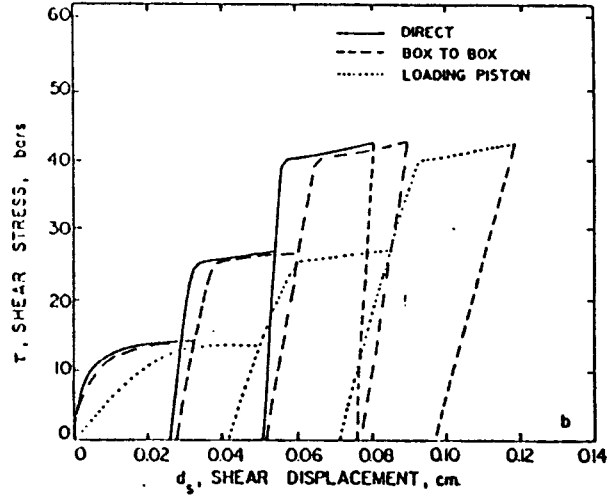
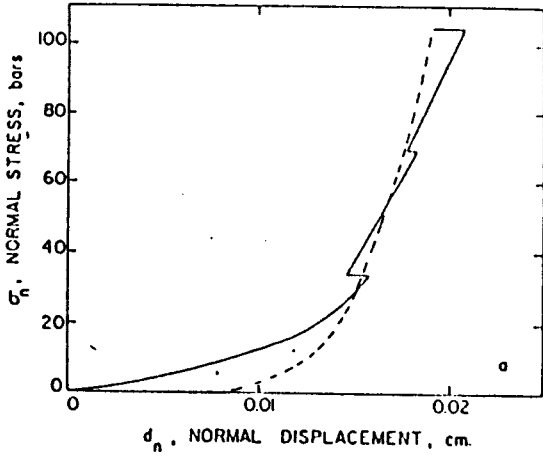
Typical results of a jointed triaxial test (see Table 1)

TABLE 1

Test Portion	σ_3 , Confining Pressure Bars	K_s , Shear Stiffness Kb/cm
1	36	3.3 ± 1.5
2	10	2.2 ± 1
3	70	9.5 ± 3

Direct Shear Tests

1) Sample with natural open fracture

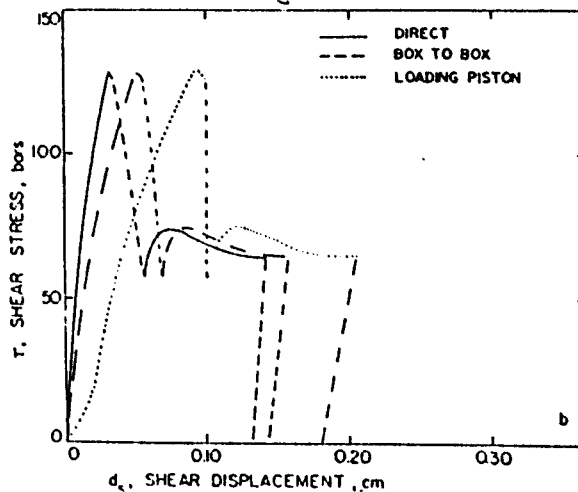
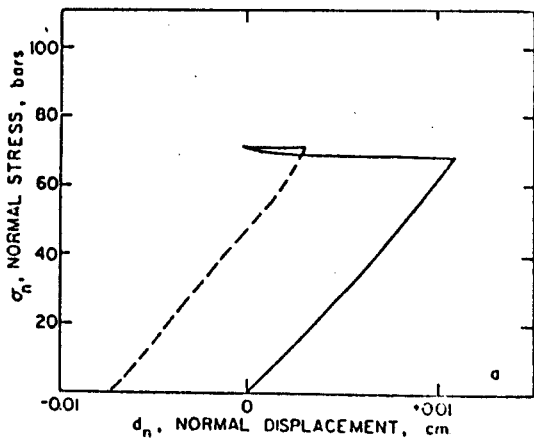


Results of a direct shear test on a rock sample containing a natural open fracture where three different measurement methods were used to determine the shear displacement (Table 2).

TABLE 2

MEASUREMENT METHOD			
σ_n bars	Loading Piston K_s Kb/cm	Box to Box K_s Kb/cm	Direct K_s Kb/cm
35	$.64 \pm .2$	$2.4 \pm .5$	$4.3 \pm .5$
70	$1.5 \pm .5$	$2.7 \pm .5$	$4.9 \pm .5$
105	$2.0 \pm .5$	$3.2 \pm .5$	$7.6 \pm .5$

2) Sample with a natural intact joint



Results of a direct shear test on a rock sample containing a natural intact joint where three different measurements methods were used to determine the shear displacement (See Table 3).

TABLE 3

Measurement Method	σ_n bars	K_s Kb/cm
Loading piston	70	$2.7 \pm .5$
Box to box	70	5.2 ± 1
Direct	70	8.1 ± 2

Comparison of in-situ shear and normal stiffness with laboratory results : see Tables 4 and 5.

TABLE 4

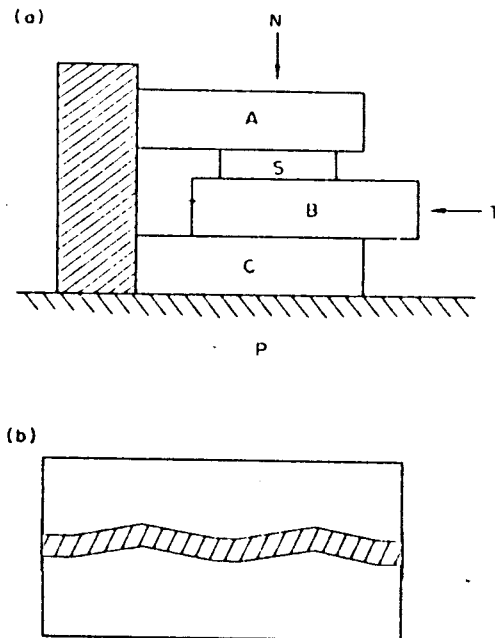
SHEAR STIFFNESS					
Direct Shear		Jointed Triaxial		In-situ	
σ_n bars	K_s Kb/cm	σ_n bars	K_s Kb/cm	σ_n bars	K_s kb/cm
35	$4.3 \pm .5$	10-27	2.2 ± 1	0-12	1.6 ± 1
70	$4.9 \pm .5$	35-85	3.3 ± 1.5	0-28	1.2 ± 1
105	$7.6 \pm .5$	70-180	9.5 ± 3	0-63	4.8 ± 1.5

TABLE 5

NORMAL STIFFNESS		
	Direct Shear K_n Kb/cm	Jointed Triaxial K_n Kb/cm
First loading	$0.85 \pm .2$	$3.8 \pm .5$
Second loading	8.0 ± 1	9.5 ± 1
Third loading	10.1 ± 1	9.5 ± 1

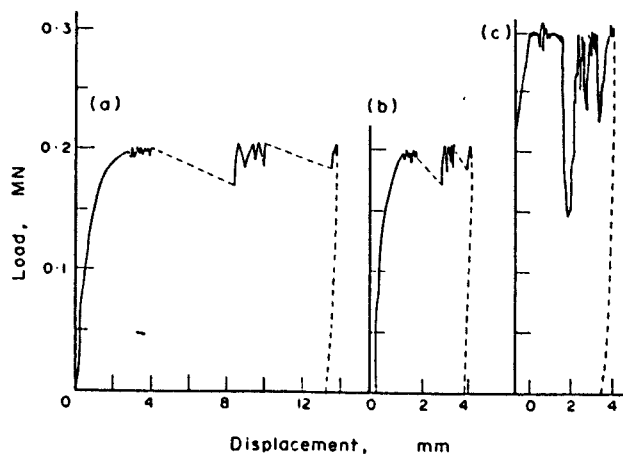
Jaeger and Gay (1974) : Shearing of compacted granular material between steel platens.

Experimental set up with (a) flat platens or (b) shaped platens.



(a) Diagram of arrangement of shearing compacted material. In an alternative arrangement a second specimen is placed between the platens B and C.

(b) Cross-section of the 'shaped' platens used in some experiments. The shaped area represents the samples, which is held in place during compaction by masking tape.



Load-displacement curves for shearing of a crushed marble-mica schist mixture enclosed in a ring of salt (size range 178-355 μm), flat platens; dashed lines indicate displacement during restroking cycles. (a) Tangential load - tangential displacement; (b) tangential load - normal displacement; (c) normal load - normal displacement.

Note occurrence of stick slip events. Once sliding is initiated stick slip continues with increasing magnitude.

APPENDIX 2 : CONVERSION FACTORS

	Imperial	Metric	SI
Length	1 mile	1.609 km	1.609 km
	1 ft	0.3048 m	0.3048 m
	1 in	2.54 cm	25.40 mm
Area	1 mile ²	2.590 km ²	2.590 km ²
	1 acre	0.4047 hectare	0.4047 hectare
	1 ft ²	0.0929 m ²	0.0929 m ²
	1 in ²	6.452 cm ²	6.452 cm ²
Volume	1 yd ³	0.7646 m ³	0.7646 m ³
	1 ft ³	0.0283 m ³	0.0283 m ³
	1 ft ³	28.32 litres	0.0283 m ³
	1 UK gal.	4.546 litres	4546 cm ³
	1 US gal.	3.785 litres	3785 cm ³
	1 in ³	16.387 cm ³	16.387 cm ³
Mass	1 ton	1.016 tonne	1.016 Mg
	1 lb	0.4536 kg	0.4536 kg
	1 oz	28.352 g	28.352 g
Density	1 lb/ft ³	16.019 kg/m ³	16.019 kg/m ³
Unit weight	1 lb/ft ³	16.019 kgf/m ³	0.1571 kN
Force	1 ton f	1.016 tonne f	9.964 kN
	1 lb f	0.4536 kg f	4.448 N
Pressure or stress	1 ton f/in ²	157.47 kg f/cm ²	15.44 MPa
	1 ton f/ft ²	10.936 tonne f/m ²	107.3 kPa
	1 lb f/in ²	0.0703 kg f/cm ²	6.895 kPa
	1 lb f/ft ²	4.882 kg f/m ²	0.04788 kPa
	1 standard atmosphere	1.033 kg f/m ²	101.325 kPa
	14.495 lb f/in ²	1.019 kg f/cm ²	1 bar
	1 ft water	0.0305 kg f/cm ²	2.989 kPa
1 in mercury	0.0345 kg f/cm ²	3.386 kPa	
Permeability	1 ft/year	0.9659 x 10 ⁻⁴ cm/s	0.9659 x 10 ⁻⁴ m/s
Rate of flow	1 ft ³ /s	0.02832 m ³ /s	0.02832 m ³ /s
Moment	1 lbf ft	0.1383 kgf m	1.3558 Nm
Energy	1 ft lbf	1.3558 J	1.3558 J
Frequency	1 c/s	1 c/s	1 Hz

SI Unit Prefixes

Prefix	tera	giga	mega	kilo	milli	micro	nano	pico
Symbol	T	G	M	k	m	μ	n	p
Multiplier	10^{12}	10^9	10^6	10^3	10^{-3}	10^{-6}	10^{-9}	10^{-12}

SI Symbols and Definitions

N	=	Newton	=	kg m/s^2
Pa	=	Pascal	=	N/m^2
J	=	Joule	=	m.N